



球状トカ马克における 加熱・制御技術

高瀬雄一
東京大学 大学院新領域創成科学研究科

第13回 若手科学者によるプラズマ研究会
(プラズマ加熱・制御技術の進展と展望)

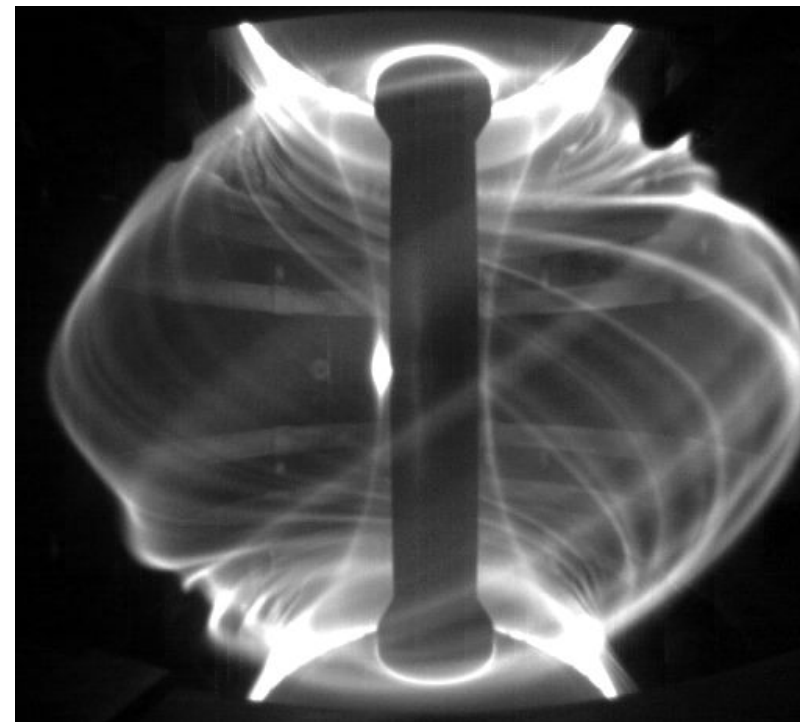
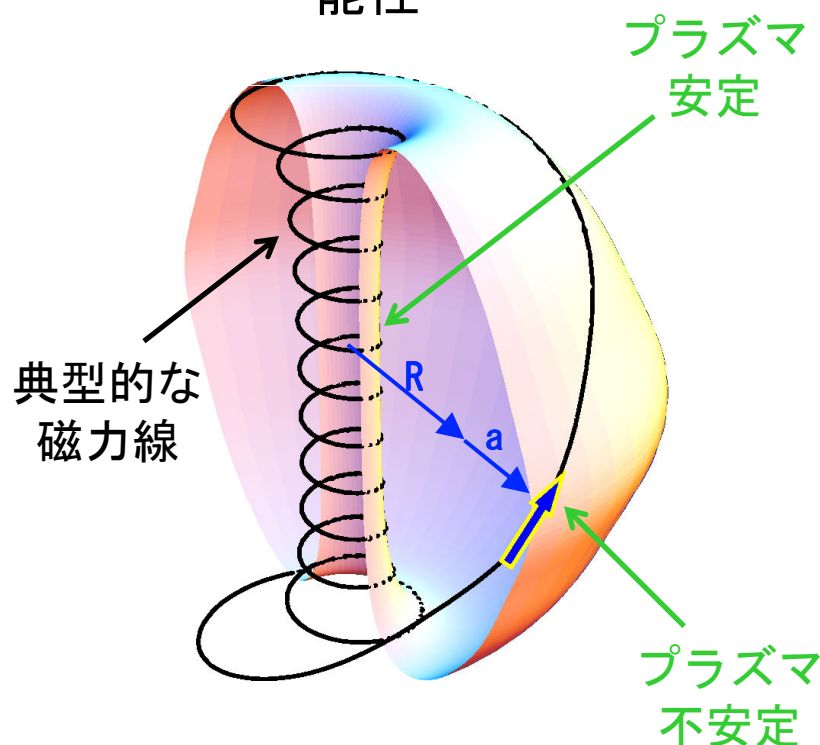
2010年3月10-12日
日本原子力研究開発機構 那珂核融合研究所

球状トカマク (ST) とは

ST

- ・ アスペクト比の低いトカマク ($A < 2$ 程度)
- ・ 小型装置で閉じ込めのよい高 β プラズマが実現可能

→ 小型の燃焼プラズマ装置・核融合実証炉（デモ炉）実現の可能性



U.S. STCC Selected Three Mission Options, Taking Advantage of Attractive ST Features



Three ST missions to advance fusion energy science during the ITER Era (~20 years)

- **High-Q Burning Plasma (BP)**

Explore strongly coupled nonlinear plasma conditions ($f_{BS} \rightarrow 1$, $\beta \rightarrow$ ideal wall limit, etc.) prototypical of DEMO.

- **Fusion Nuclear Science (FNS)**

Elucidate and resolve synergistic effects in science of fusion plasma and neutron material interactions, fuel cycle & power extraction in full fusion nuclear environment up to 1 MW-yr/m².

- **Plasma Material Interface (PMI)**

Qualify candidate PFCs in long-pulse DD facility approaching conditions of a fusion nuclear device.

[STCC Report, 12/12/09, "Shared Documents" @ https://info.ornl.gov/sites/us_stcc/default.aspx]

Attractive Features

- **Plasma:** high β_T limits, $\tau_{Ei} (>>\tau_{Ee})$, q_{CYL}
- **Device:** small (size \times field \times $P_{FUS} \times P_{aux}$); high Φ_{DIV} , W_L
- **Discovery:** extend toroidal plasma regime and enhance understanding

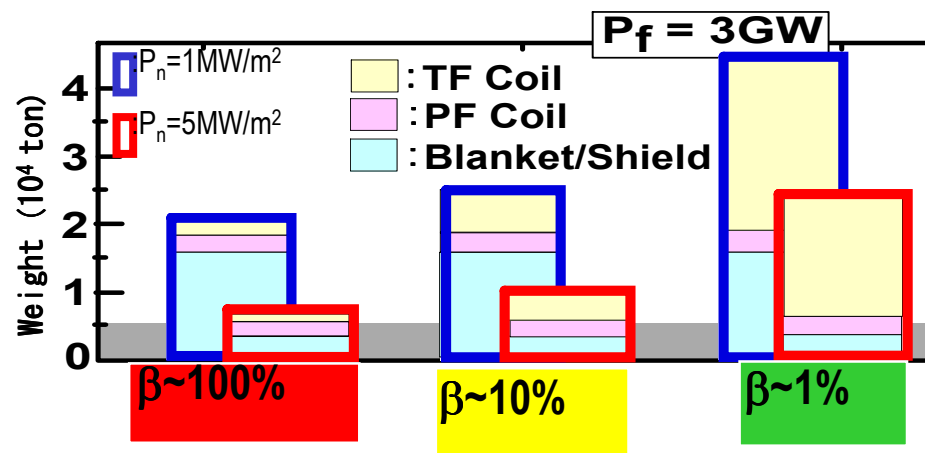
	PMI	FNS	BP
Q	0.01	0.8-1.5	10-20
P_{FUS} (MW)	0.2	19-75	300
R (m)	1.2	1.3	1.5
I_p (MA)	3-4	4-7	9-17
q_{CYL}	3	4-6	3
β_N	≤ 3	2-3.3	5-7
W_L (MW/m ²)	-	0.3-1.0	3
Φ_{DIV} (MW/m ²)	varied	≤ 10	varied

核融合炉の効率を高めるにはどうすればよいか？



核融合出力密度

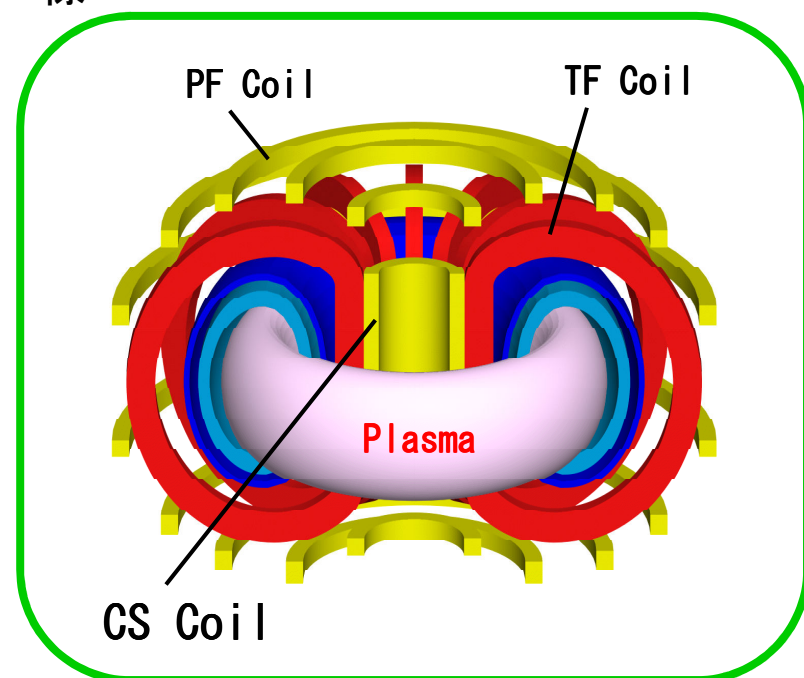
$$p_f \propto \beta^2 \cdot B_0^4$$



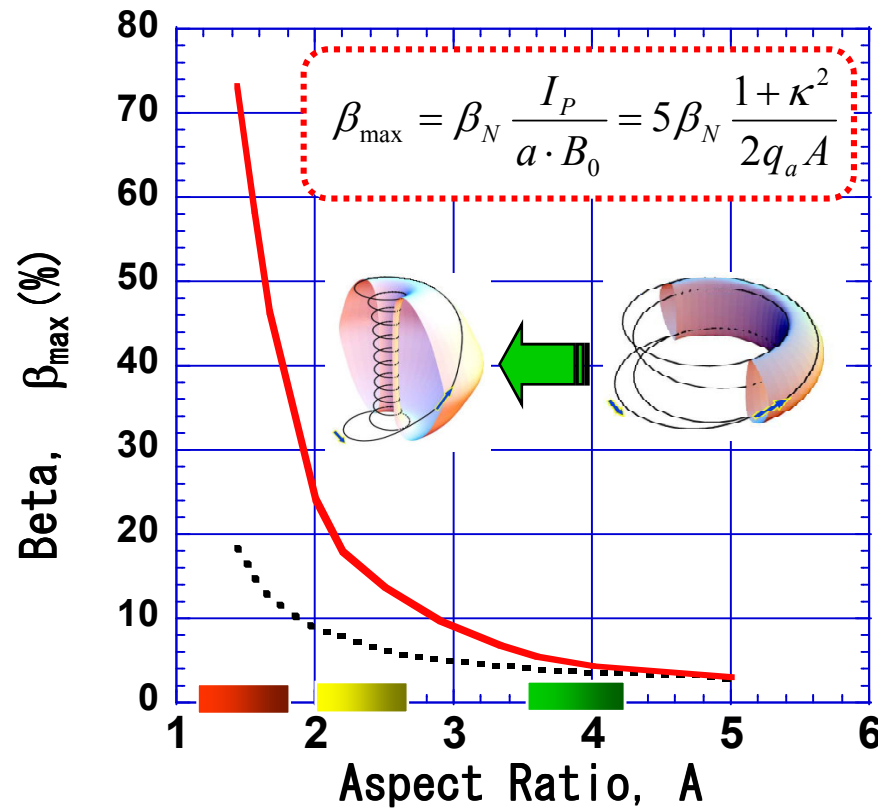
閉じ込め磁場 B_0 を高めるのではなく、
 β を高める方が経済的に有利
→ 高 β 化

$\beta = \text{プラズマ圧力} / \text{磁場圧力}$

磁場がプラズマ閉じ込めにどれだけ有効に使われているかを表す指標

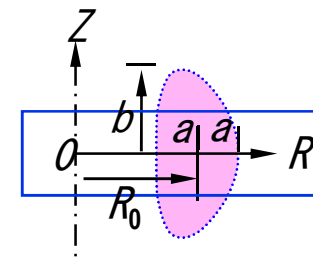


β を高めるにはどうすればよいか？



- : with CS Coil & Thick Shield (SC TFC)
- : without CS Coil & Thick Shield (SC TFC)
- : without CS Coil & Thin Shield (Copper TFC)

$$\beta_{\max} = \beta_N \frac{I_P}{a \cdot B_0} = 5 \beta_N \frac{1 + \kappa^2}{2 q_a A} \quad \beta_N = f(\kappa, A) \quad \kappa = g(A)$$

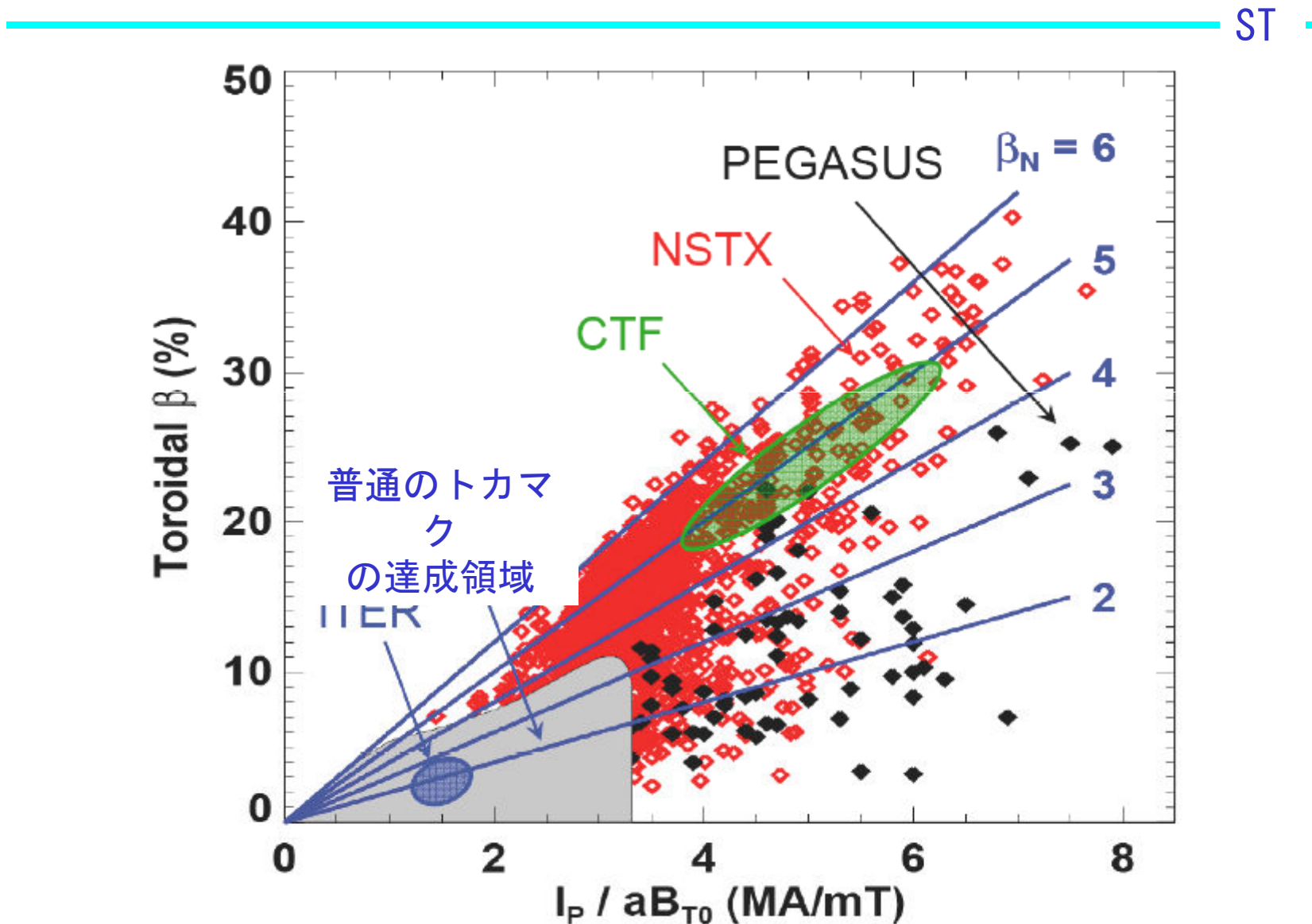


アスペクト
比
 $A = R_0 / a$

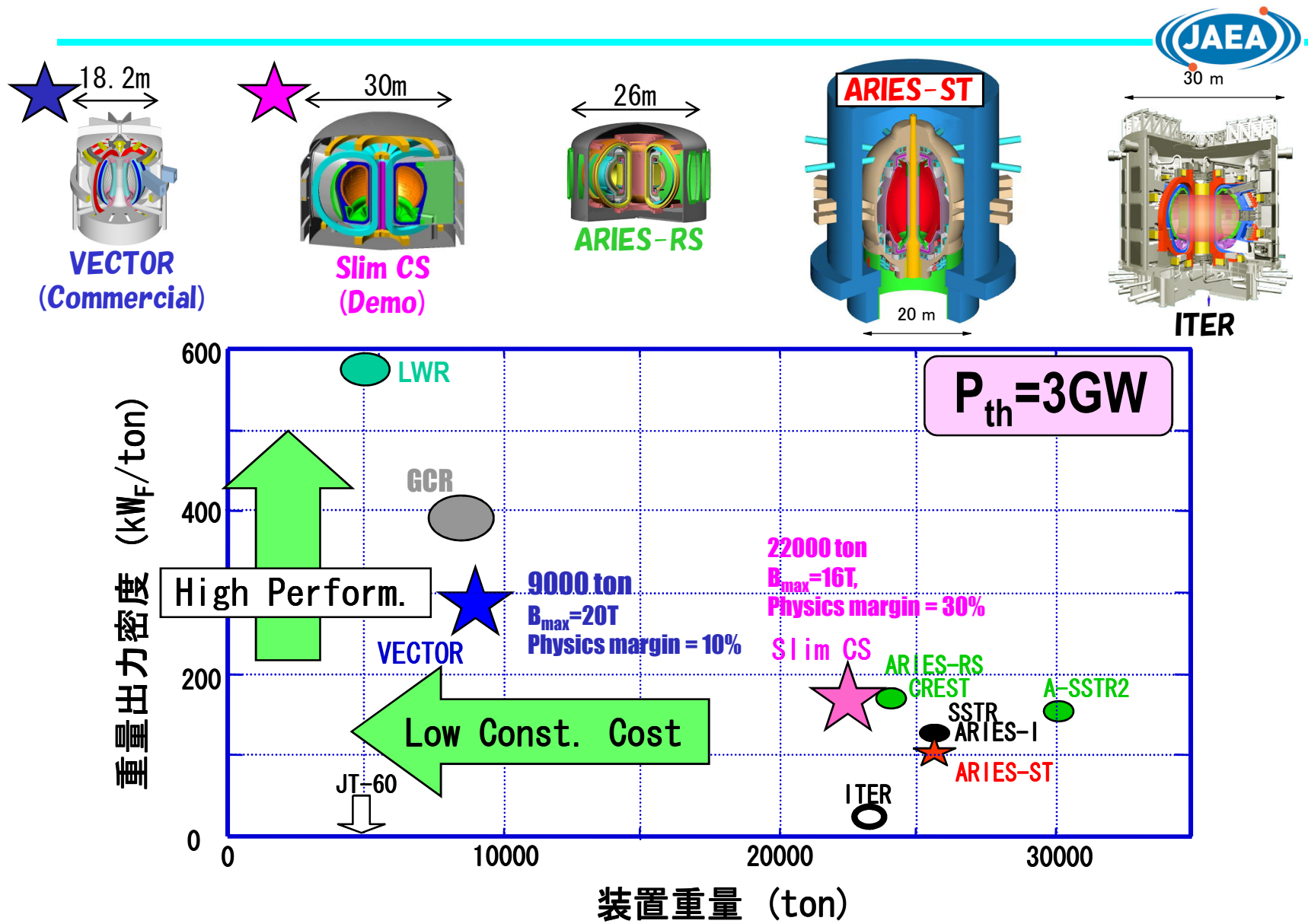
A をできる限り小さくすればよい
→ 球状トカマク

但し技術的制約より、アスペクト比はいくらでも小さくできるわけではない。

STによる高 β プラズマ安定性の実証



デモ炉と商業炉の設計例



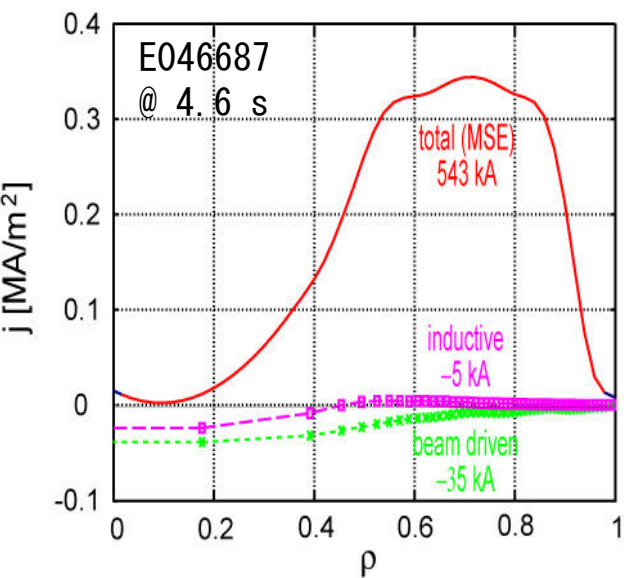
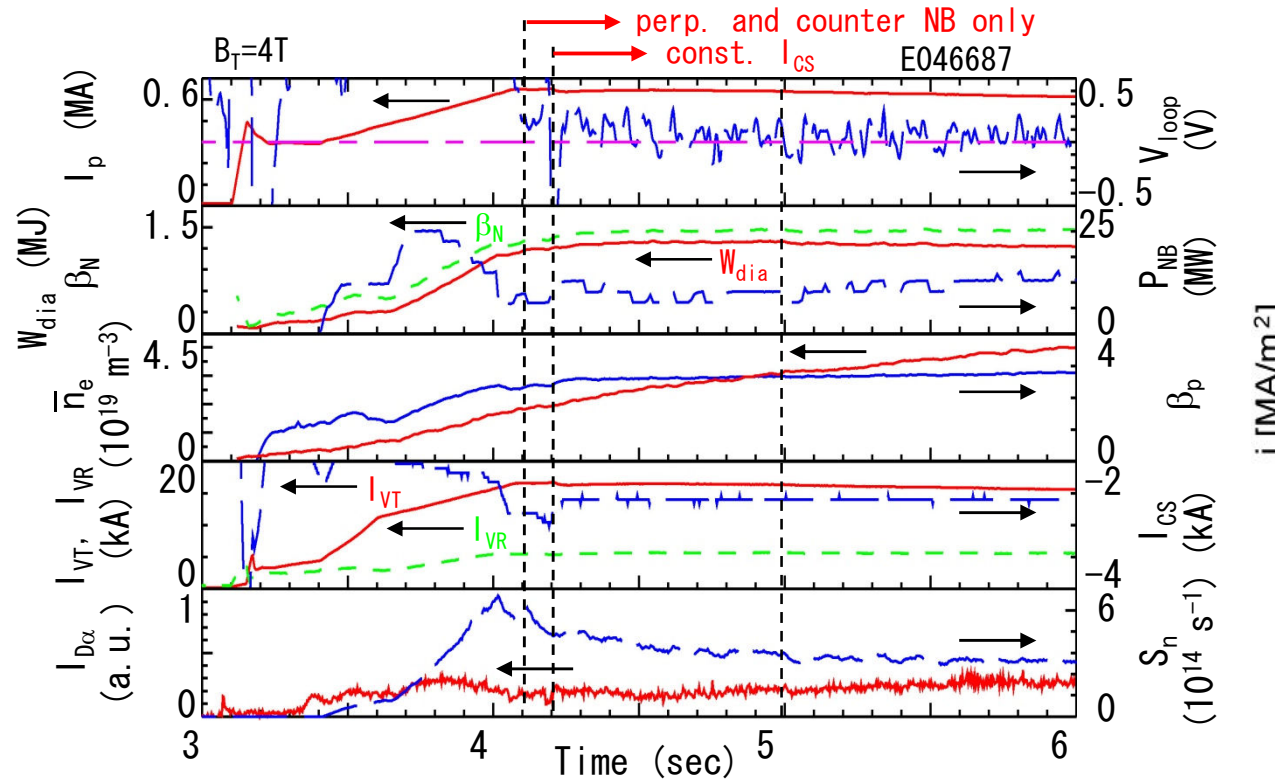
Nearly constant current (~ 0.54 MA) is maintained by BS current with constant I_{CS} and counter-NBCD current for > 0.5 sec.

Fully bootstrap-driven plasma ($f_{BS} \sim 100\%$) is realized.

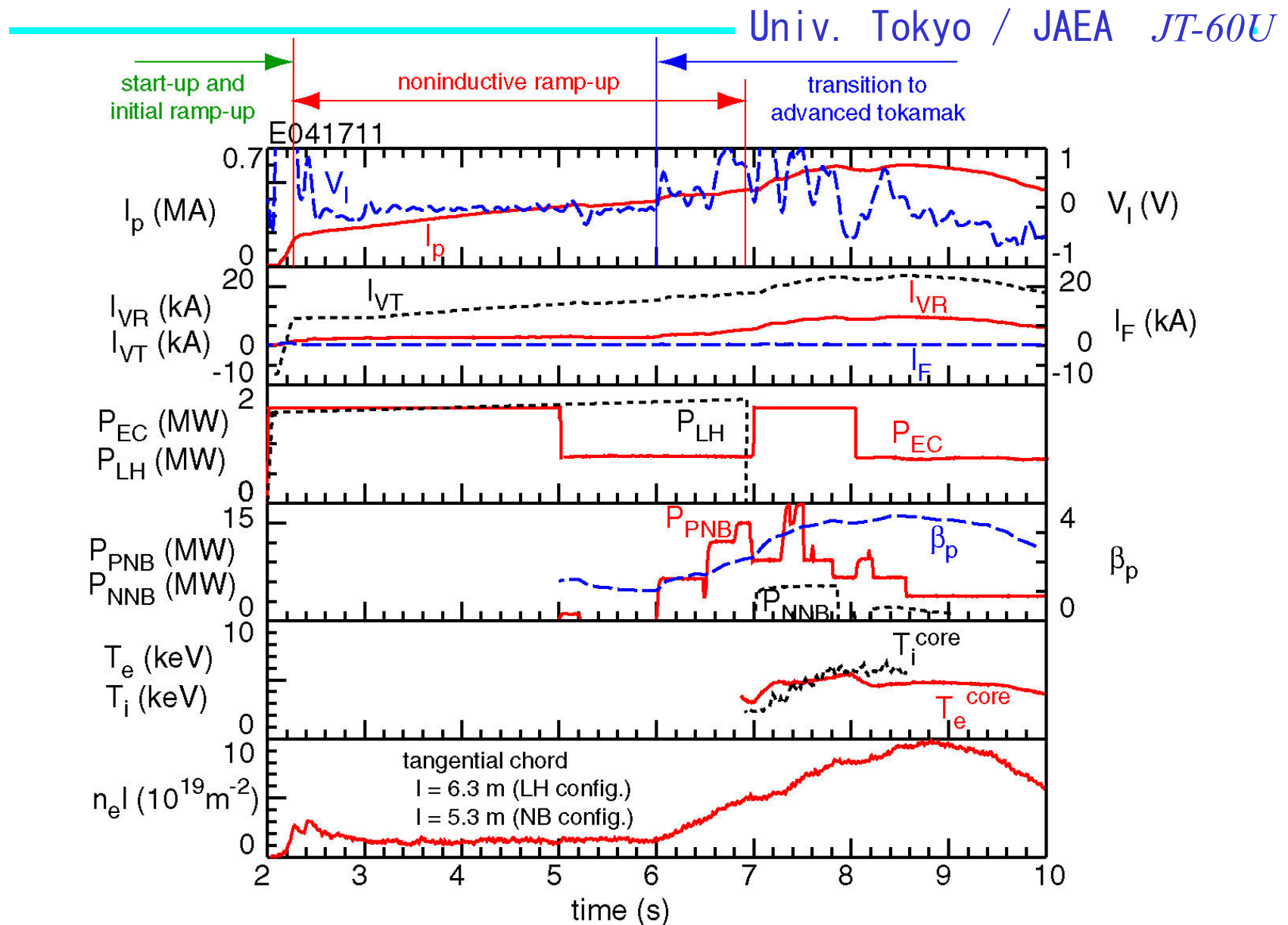
Internal loop voltage $V_{loop}(r) \sim 0$ V, $I_{tot} = 543$ kA, $I_{ind} = -5$ kA, $I_{BD} = -35$ kA,

- Duration ~ 5.8 sec self-sustained phase is limited by slow confinement degradation.

Both W_{dia} and I_p decrease gradually after 5 sec.



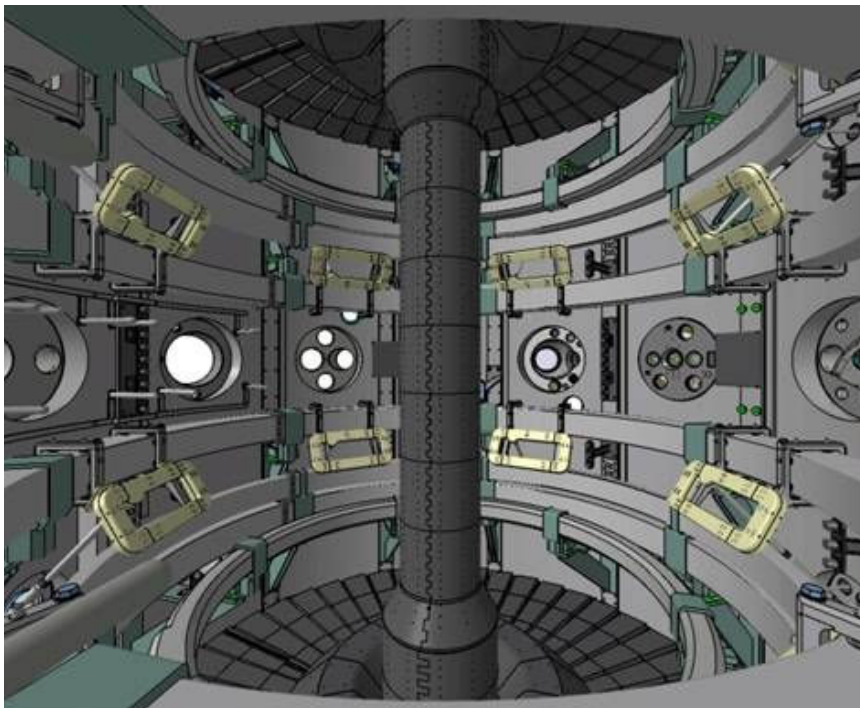
CS-less Start-up Demonstrated in JT-60U



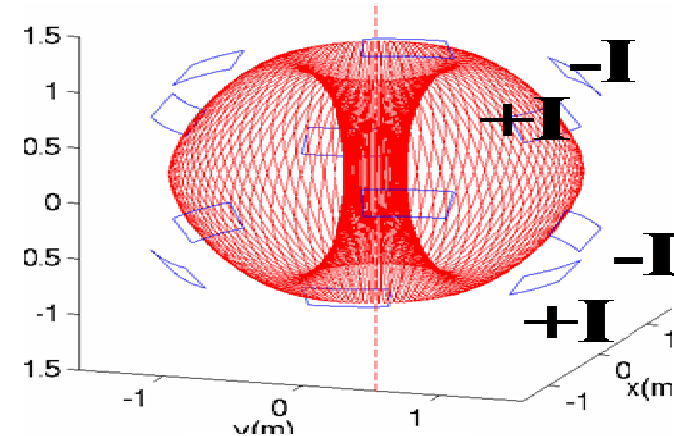
ELM control

MAST

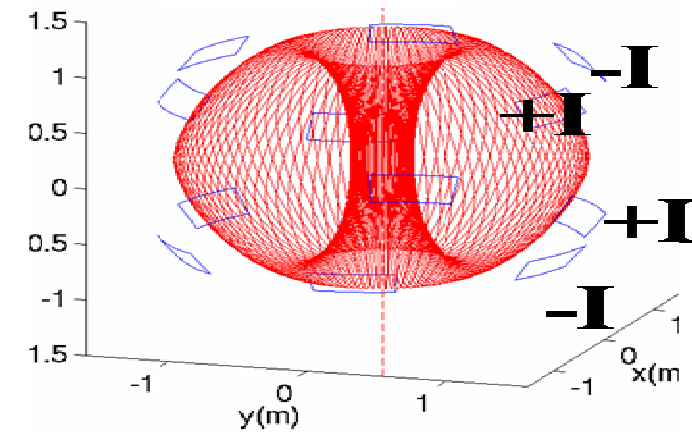
- 6 + 6 internal array - $\leq 2\text{kA}$, 4 turn coils for **ELM control** ($n = 3$).
Additional 6 coils will be installed in 2010 to allow $n = 4$, $n = 6$



Even parity



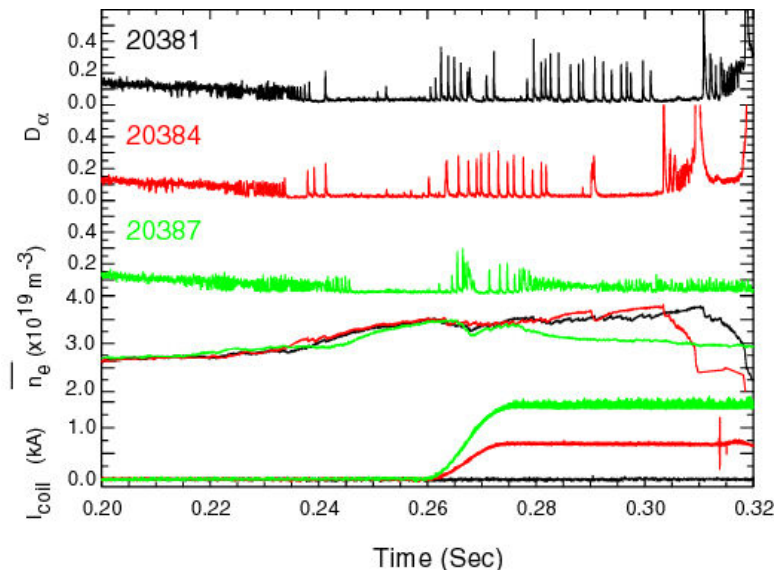
Odd parity



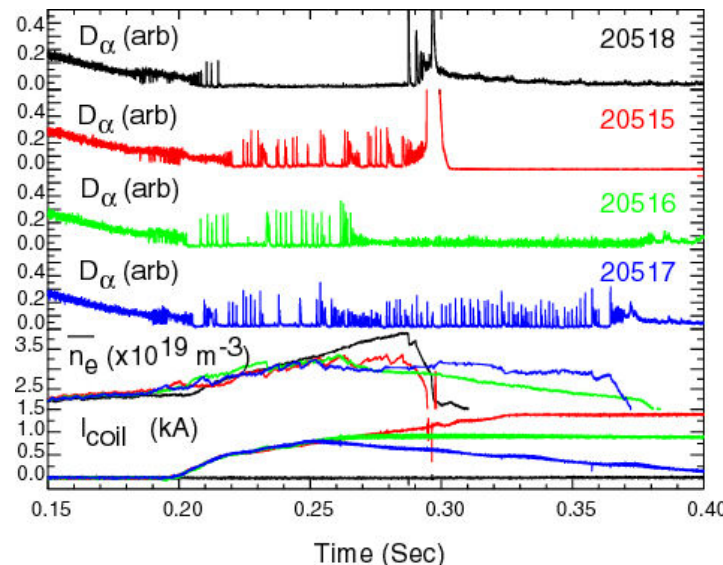
$n=3$ H-mode experiments - Type III ELMy / ELM-free H-mode

MAST

ELM character changed



ELMs stimulated in ELM-free regime



In the standard sequence for the L-H transition

L-mode – Dithering – Type III ELMs – ELM-free – Type I ELMs

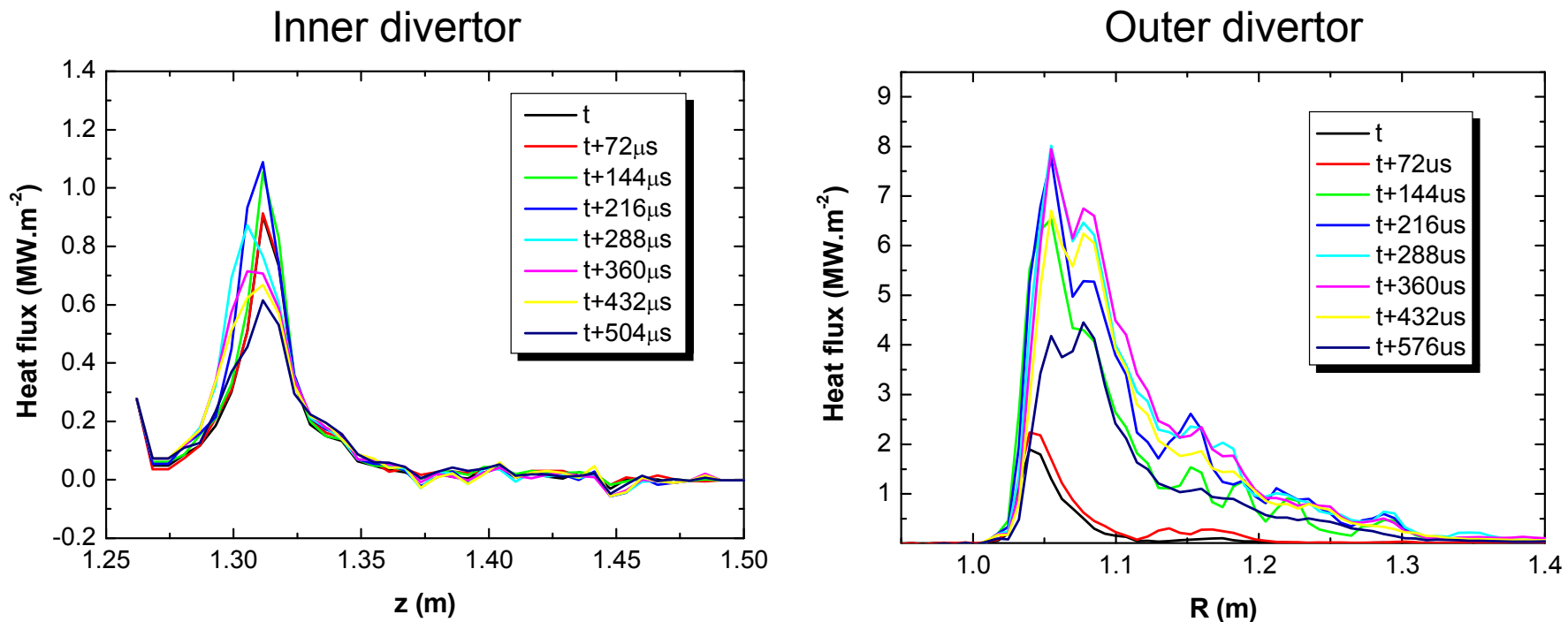
Power across separatrix P_{sep}

the application of the coils is equivalent to a small drop in P_{sep} wrt. P_{LH}

Heat flux profiles during ELMs

- ❑ Evolution of heat flux profiles during an ELM in connected DND
(1 frame every 72 ms):

MAST

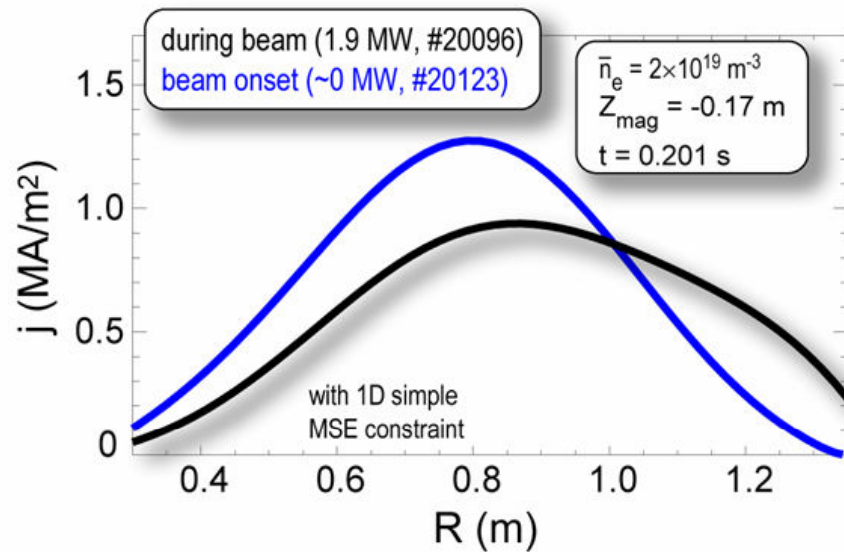


- ❑ Heat flux profile in inner divertor only slightly modified during an ELM
- ❑ Filamentary structure clearly observed in outer divertor
- ❑ E_{outer} is between 15 and 40 times higher than E_{inner}

Off-axis NBCD

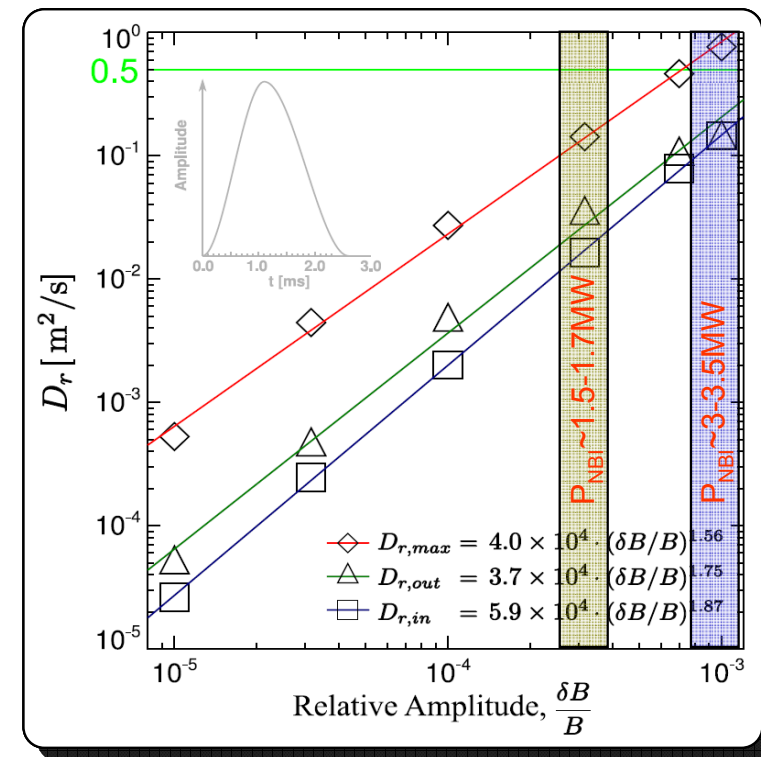
MAST

- MSE confirms $j(r)$ broadening during off-axis NBCD



- HAGIS (non-linear drift-kinetic δf code) calculations of fast ion diffusion arising from $n = 1$ fishbone activity are consistent with experiment

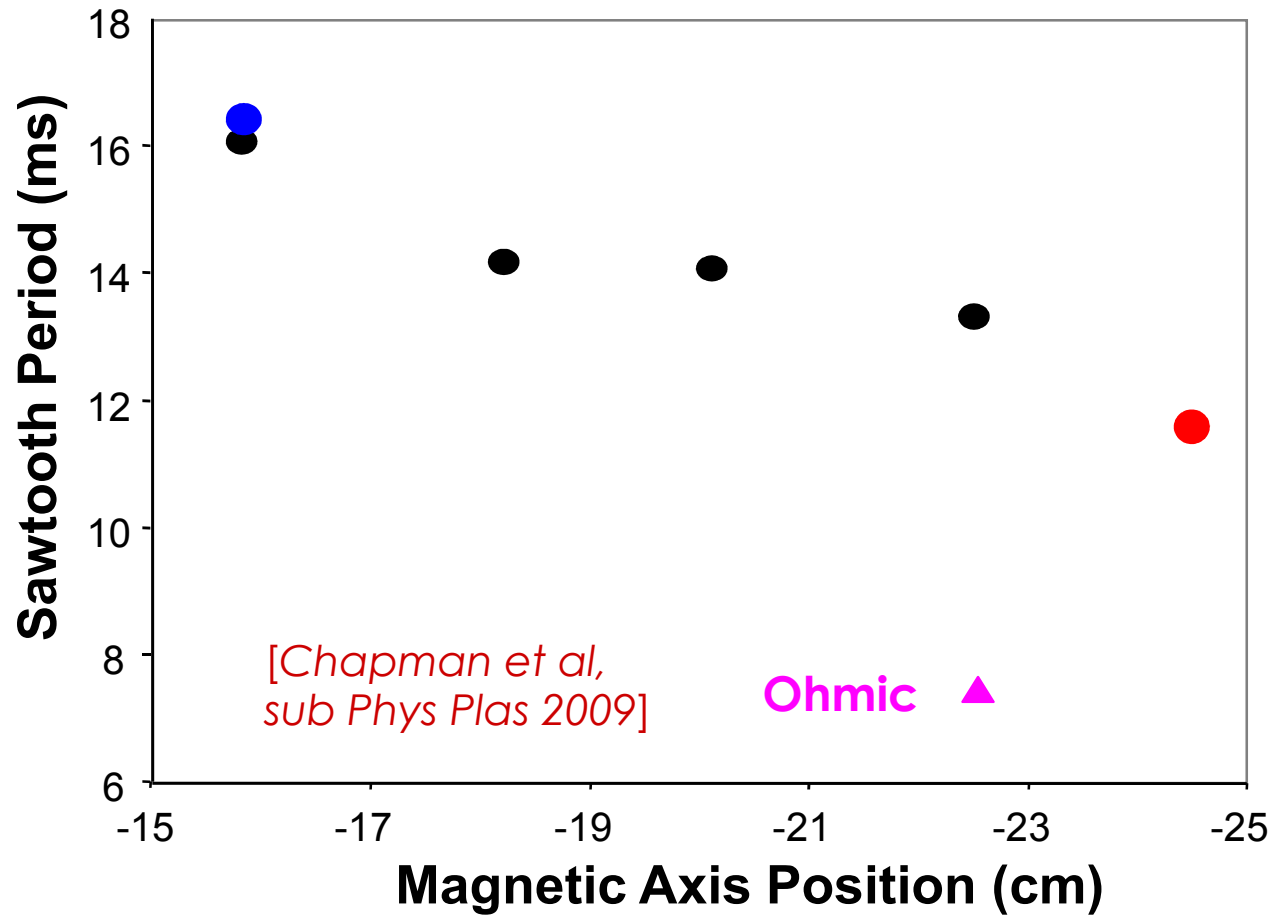
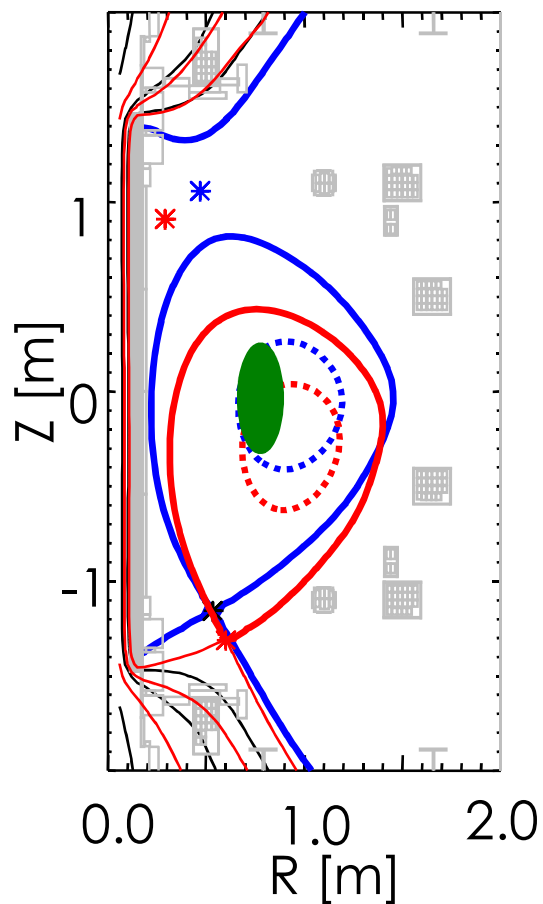
- Anomalous fast ion diffusion ($D_b \sim 0.5 \text{ m}^2/\text{s}$) needed to match neutron rate and stored energy – linked to $n = 1$ core MHD (fishbones)



Sawtooth control with off-axis NBI

- Scan the deposition location by moving plasma vertically
 - Sawtooth behaviour affected by deposition location relative to $q=1$
 - Passing ion effects dominate over change in NBCD, v_ϕ shape etc

MAST

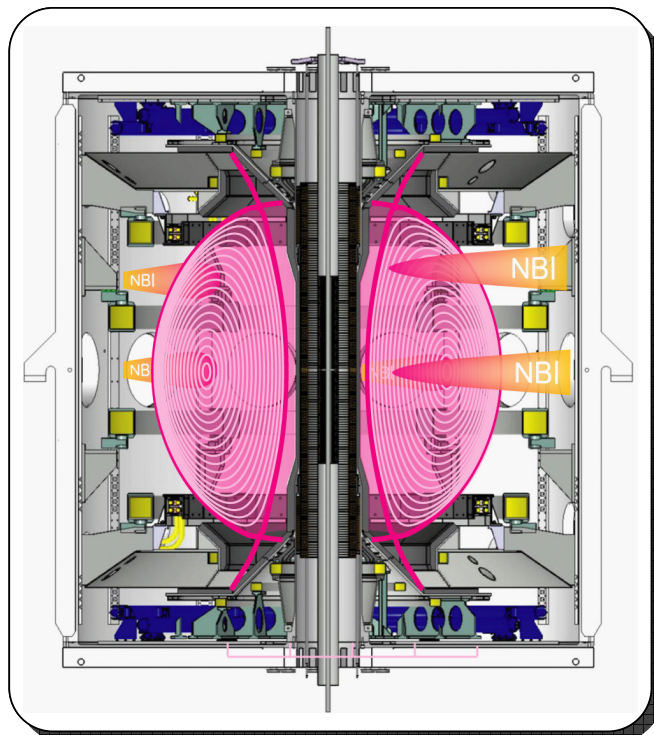


MAST Upgrade

Objectives

MAST

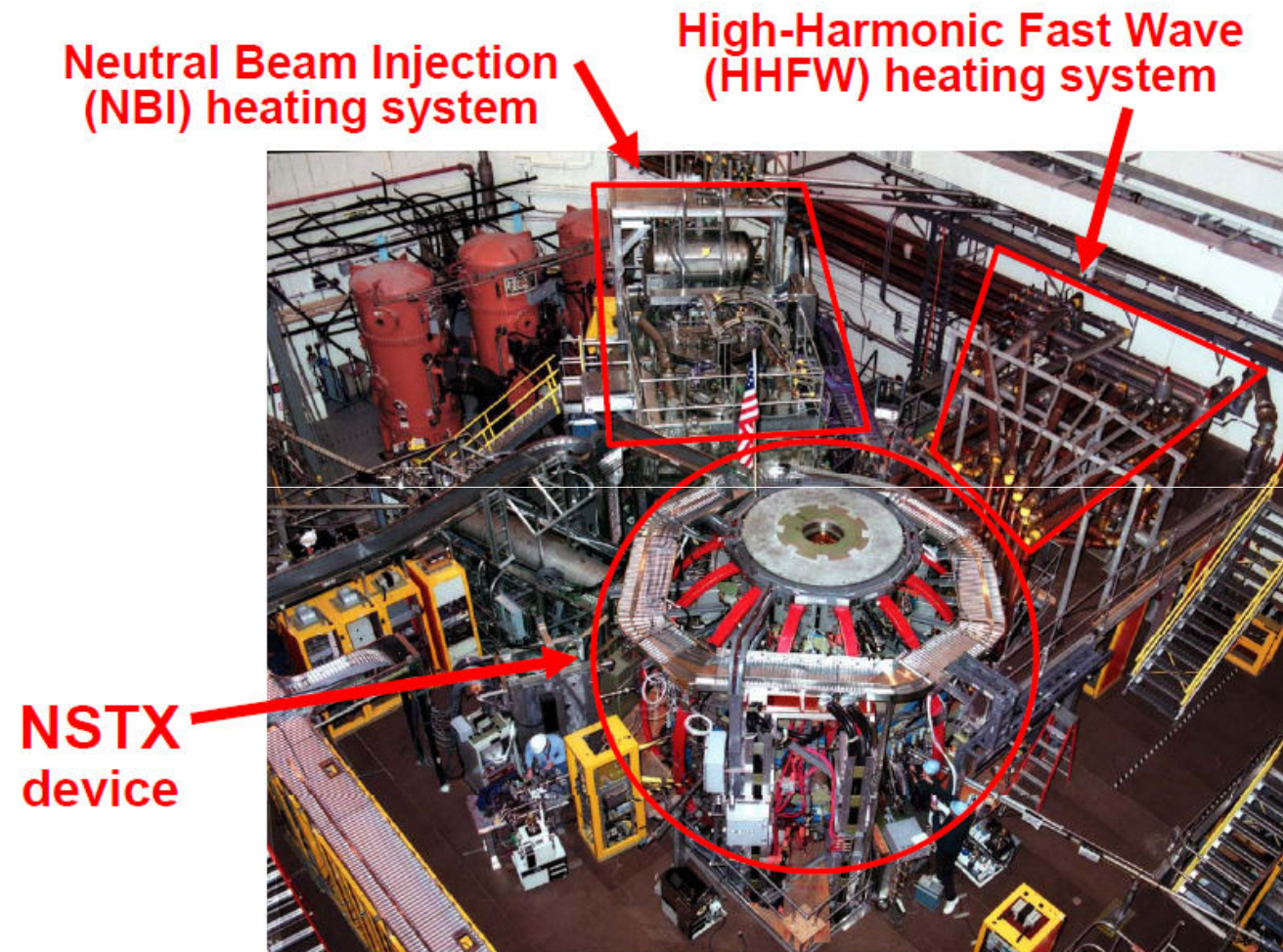
- Address gaps in the physics basis of an ST CTF
- Provide influential input to EFDA missions in support of ITER
- Contribute to development of divertor concepts for DEMO



- Increased heating power (NBI, EBW)
- adaptable system providing control of $j(r)$, $p(r)$, $v(r)$
- Relaxed current profile
- fully non-inductive operation possible
- Increased TF, increased solenoid flux
- higher current, longer pulse routine operation
- Improved exhaust and density control
- closed cryopumped divertor

NSTX is the most capable Spherical Torus (ST) in the world fusion program

NSTX



Baseline Parameters:

Major Radius 0.86 m

Minor Radius 0.66 m

Aspect Ratio 1.3-1.6

Elongation 1.8 – 3.0

Triangularity 0.2 – 0.8

Plasma Current
1 MA ($t > \tau_{\text{skin}}$)

Toroidal Field
0.35 – 0.55 T

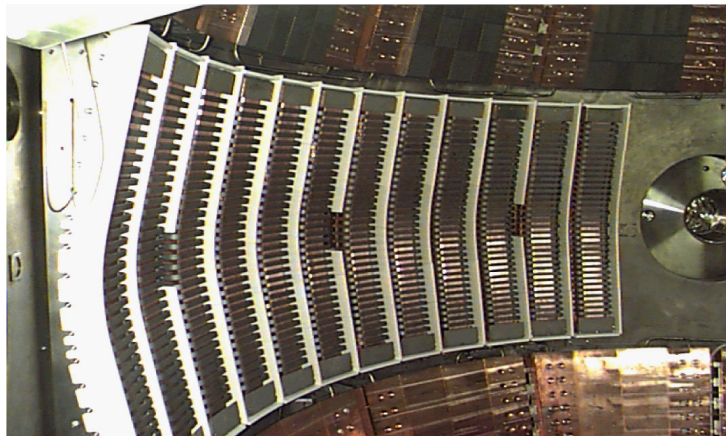
Heating and CD
7 MW NBI (2 sec)
5 MW NBI (5 sec)
3-6 MW HHFW
0.2 MA CHI

Pulse Length
~ 1 sec at 0.55 T
~ 2 sec at 0.38 T

Extensive and novel plasma diagnostics

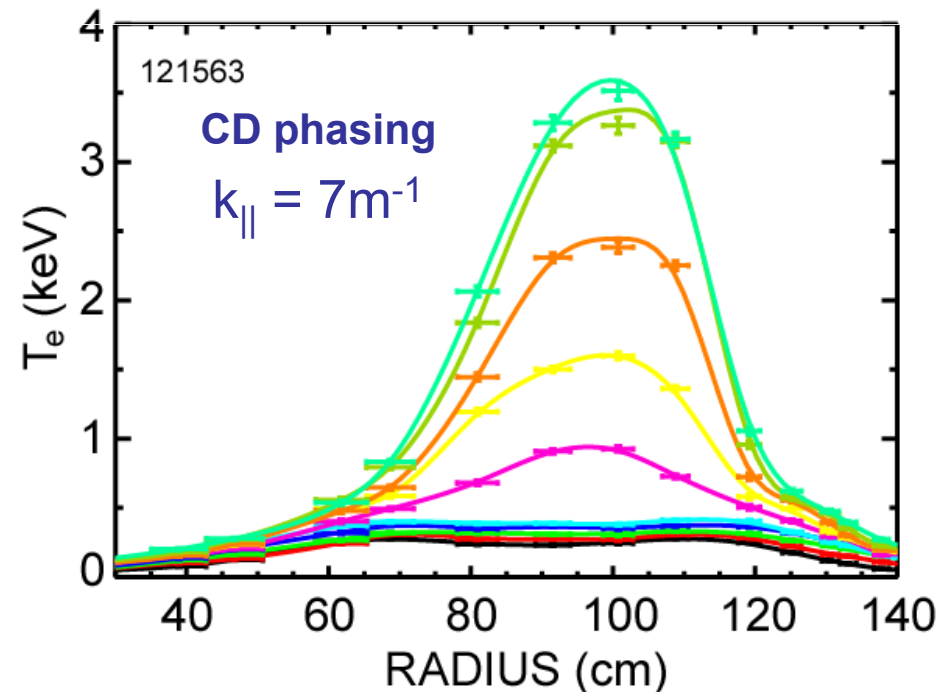
- 59 PPPL/PU researchers, 91 from 29 other U.S. institutions, 45 international

HHFW Heating Efficiency Improved with B_T



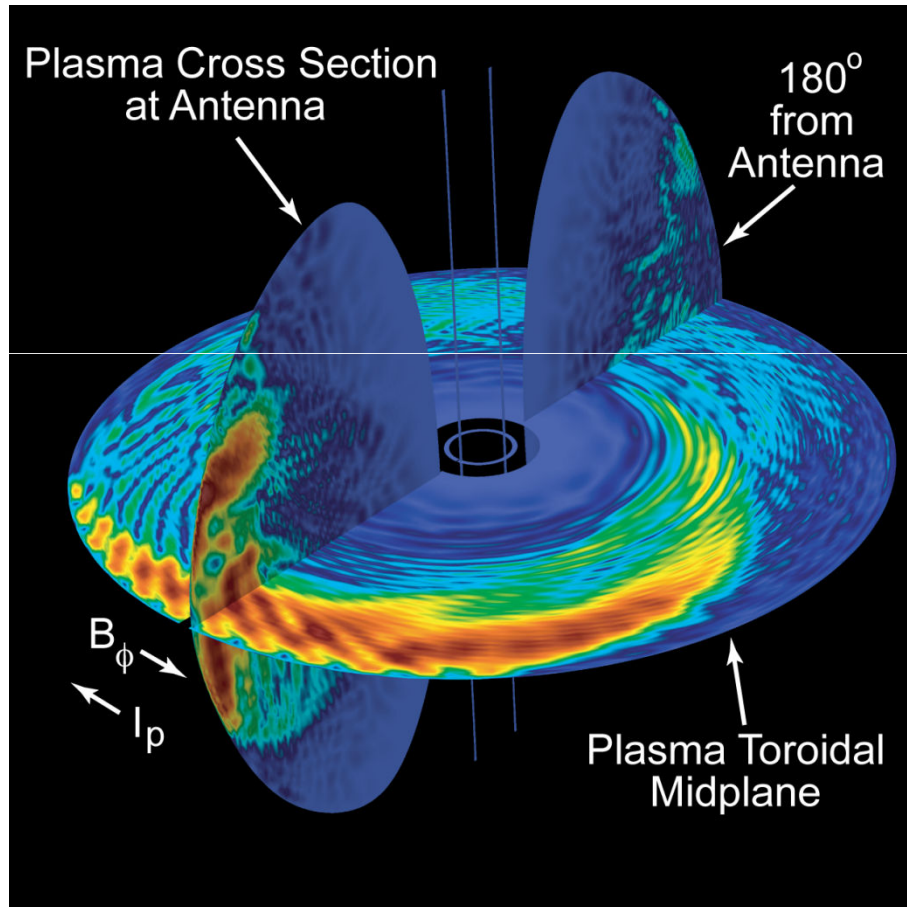
- *NSTX High-Harmonic Fast Wave (HHFW) heating and current drive research utilizes sophisticated ICRF launcher:*
- *12 strap antenna, 6MW capability*
- *6 independent transmitters*
- *Real-time control of launched k_{\parallel} from 0 to $14m^{-1}$*

- Achieved high $T_e = 3.6\text{keV}$ (nearly double the previous value) in current drive phasing for first time at $B_T = 5.5\text{kG}$
- Higher B_T and k_{\parallel} improved HHFW core electron heating - reduced edge parasitic loading



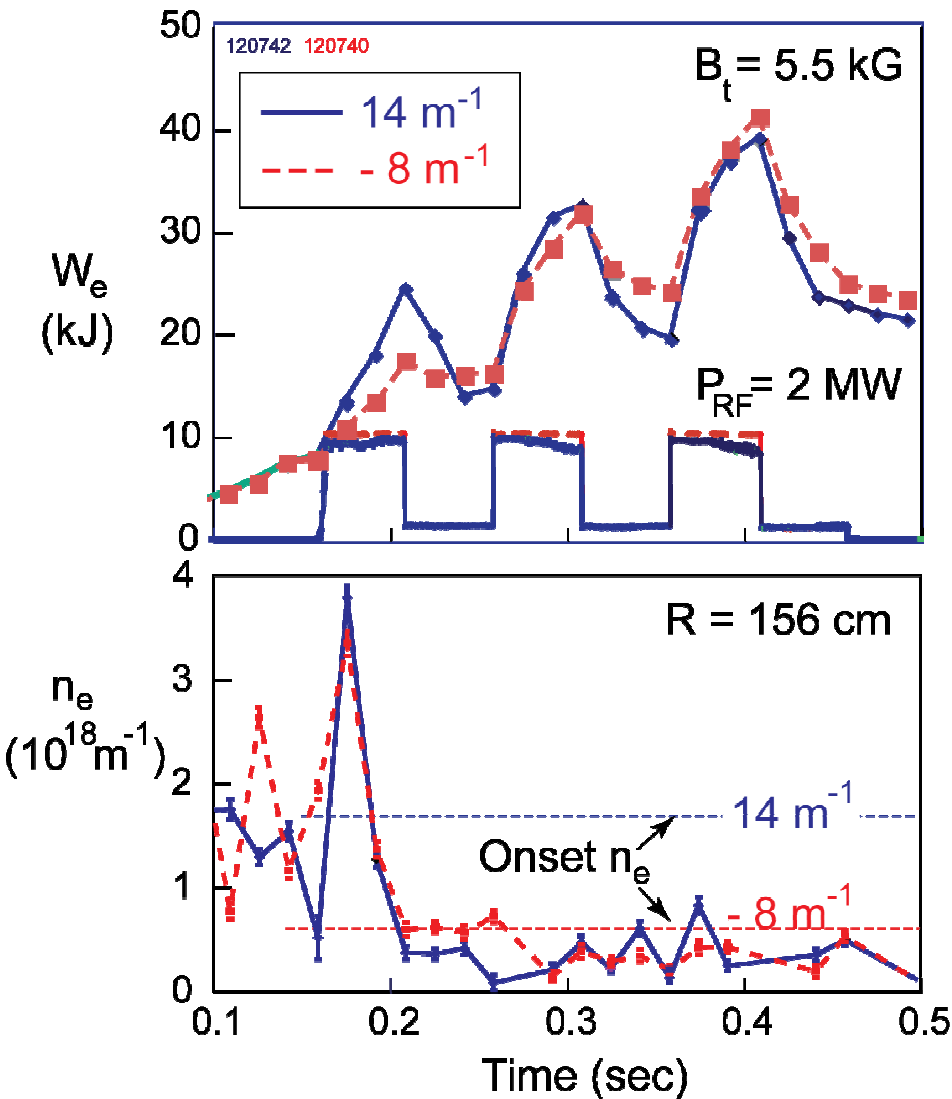
NSTX clearly separates edge HHFW losses from core deposition

AORSA $|E_{RF}|$ field amplitude for -90° antenna phase case with 101 n_ϕ



- Waves propagate around plasma axis in $+ B_\phi$ direction
– similar to GENRAY rays
- Wave fields very low near inner wall
- RF SciDAC project will include edge loss mechanisms in codes
- NSTX is good platform for benchmarking advanced RF codes

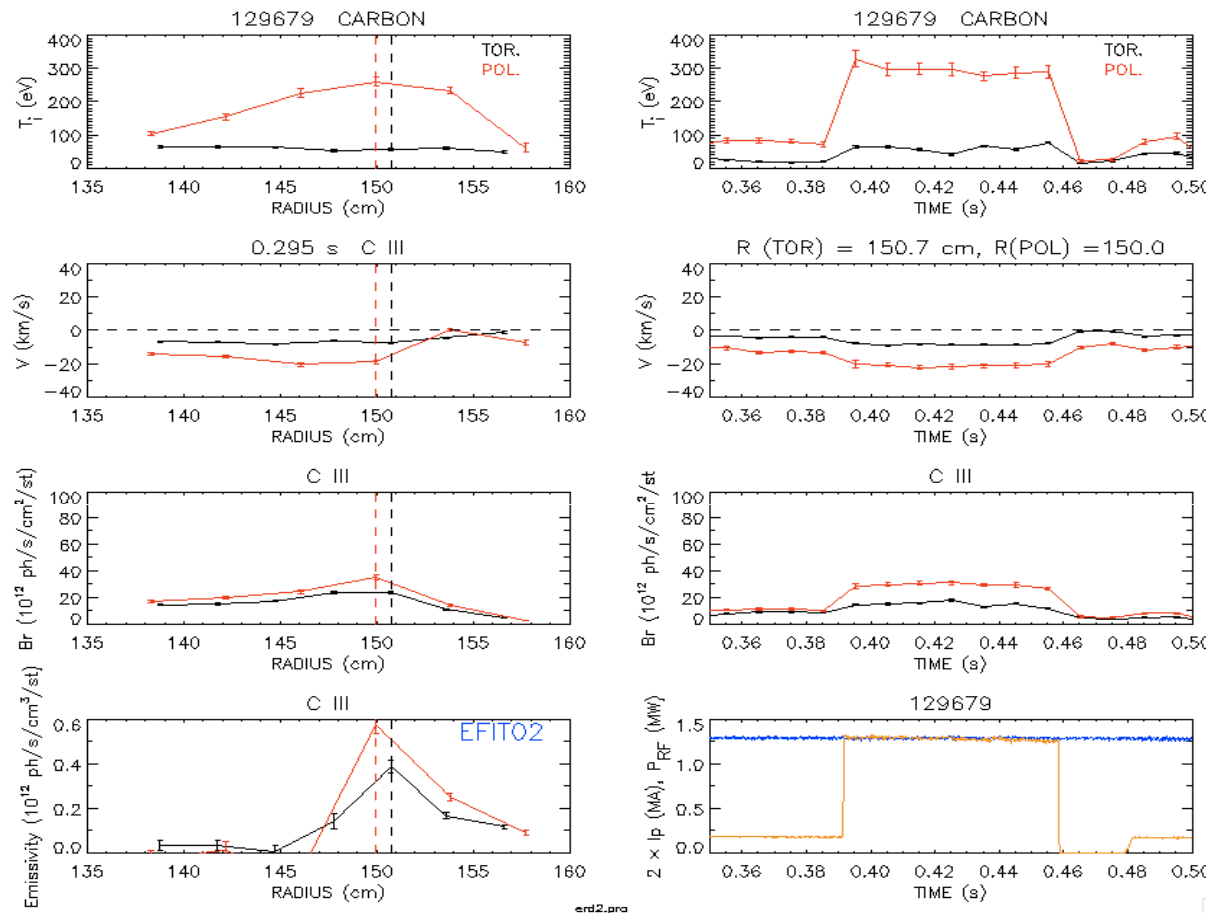
Edge power loss increases when perpendicular propagation onset density is near antenna/wall



- ΔW_e at -8 m^{-1} about half ΔW_e at 14 m^{-1} for the first pulse
- ΔW_e at -8 m^{-1} and 14 m^{-1} comparable for the last two RF pulses
- Density in plasma edge is high for first pulse and low for last two pulses
- Edge density affects heating when above onset density close to antenna, consistent with surface wave propagation near antenna/wall contributing to RF losses

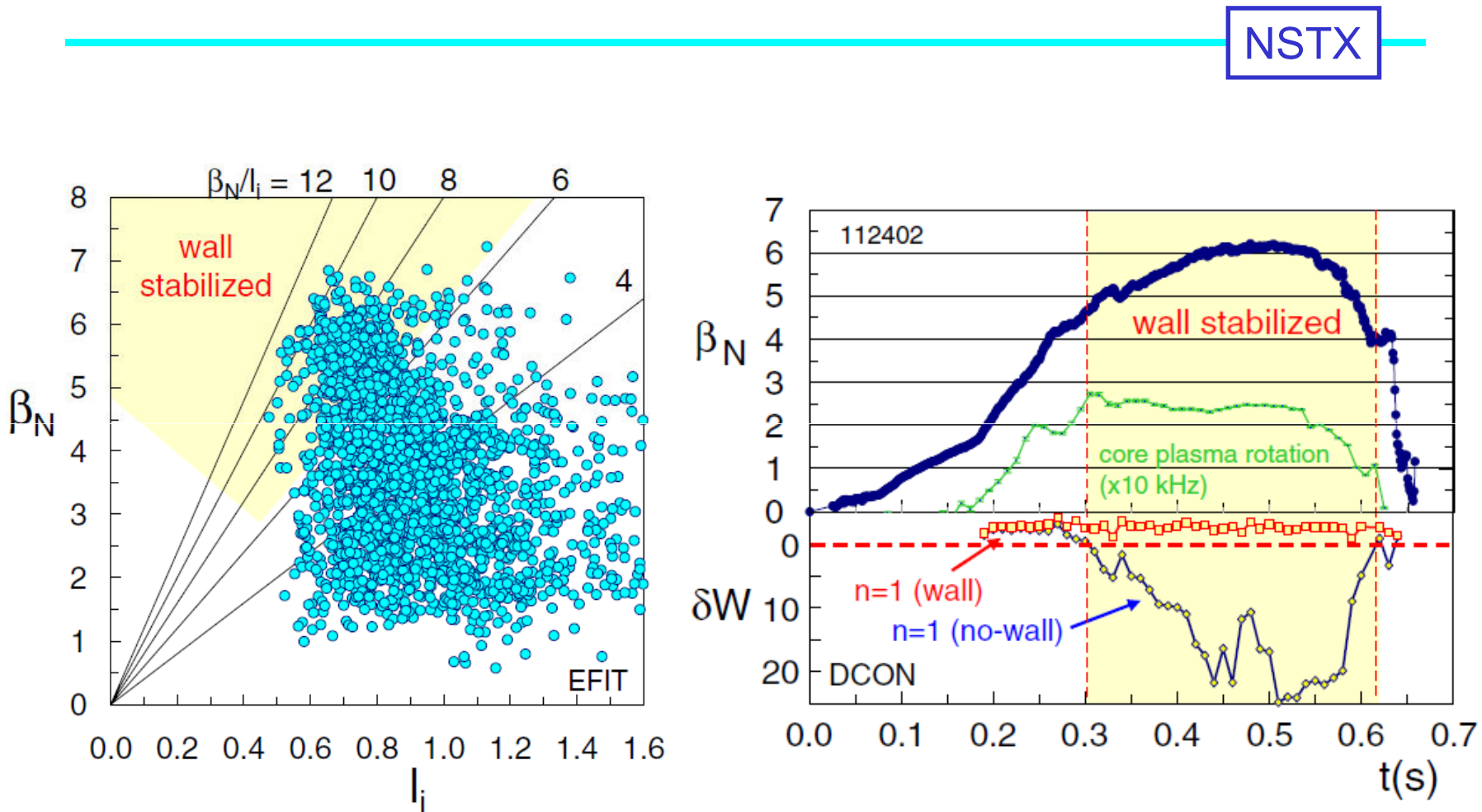
Revisiting possible parametric decay effects in plasma

edge
Poloidal heating in edge may eject energetic edge ions



- Edge ions are heated to hundreds of eV: CIII, CVI, LiII, and Helium
- Emission location for CIII and CVI is ~ 150 cm, just inside separatrix
- Edge ion heating may result in loss of energetic ions to SOL and the diver

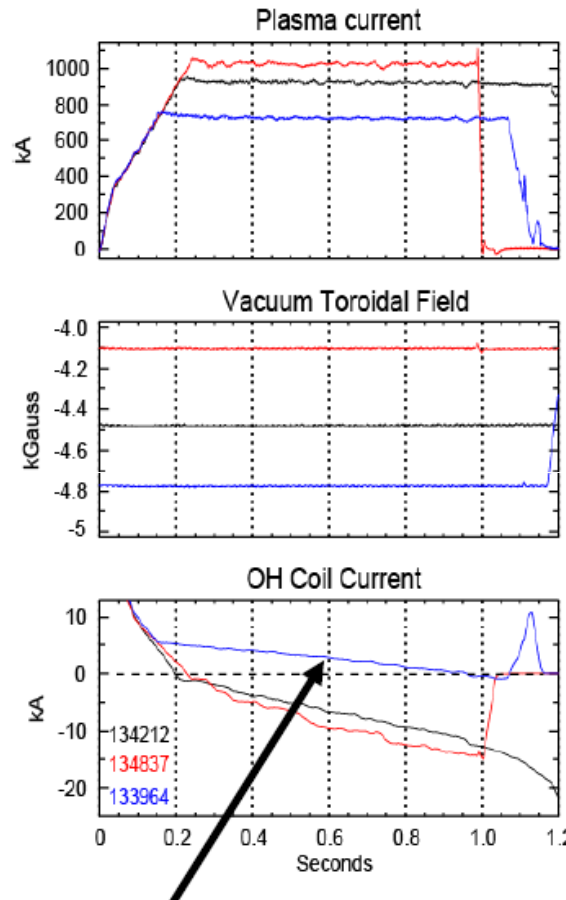
Wall-stabilized High β Plasma



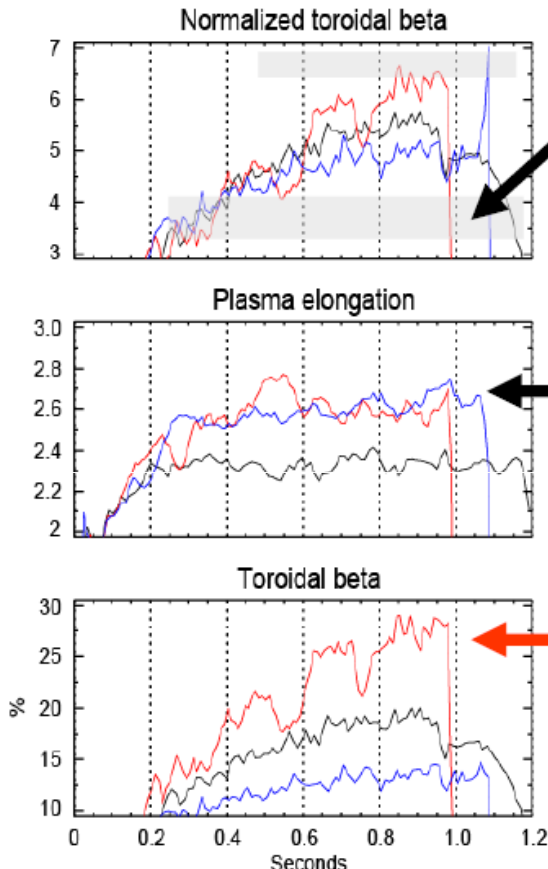
- Critical rotation velocity is consistent with Bondeson-Chu $\Omega_{\text{crit}} = \omega_A/(4q^2)$

R(09-3)

Sustained-high elongation and wall-stabilized operation has been extended from $\beta_T = 15\text{-}20\%$ to $20\text{-}30\%$



- Lowest OH flux consumption so far
 - Projects to $\sim 2\text{-}3\text{s}$ pulse



- Above $n=1$ no-wall limit for $\sim 2\tau_{CR}$

- **High elongation $\kappa = 2.6$ sustained**

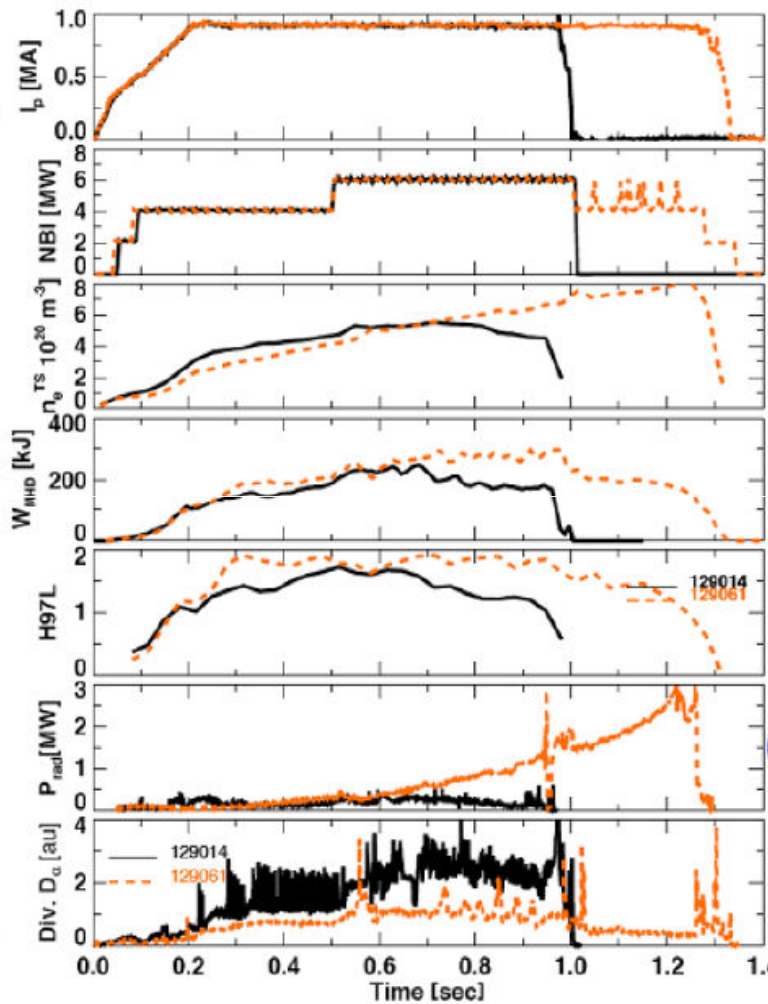
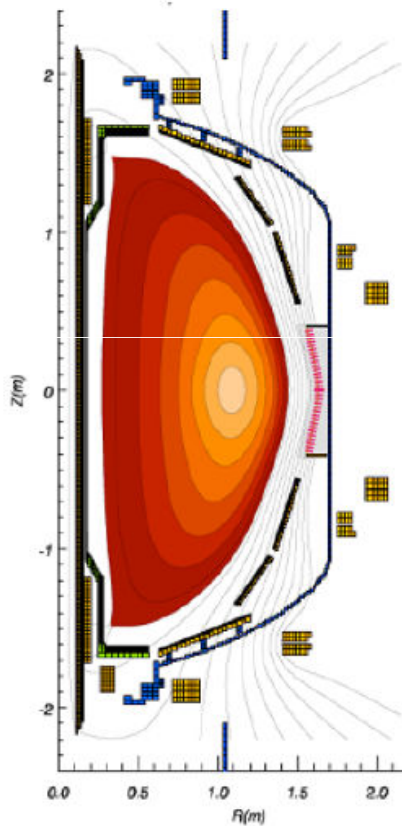
- β up to factor of 2 higher ($\beta_T = 25\text{-}30\%$)

- Pressure, density, confinement increase throughout shot

- Non-inductive fraction = 60-65%
- But, models under-predict total I_P by $\sim 20\%$
 - Non-inductive fraction could be as high as 75%
 - Investigating data uncertainties: n_e , Z_{eff} , MSE, ...

Lithium wall conditioning improves pulse length, increases τ_E , suppresses ELMs, but shows impurity accumulation

Standard high
 $\kappa \sim 2.3$, $\delta \sim 0.8$ shape

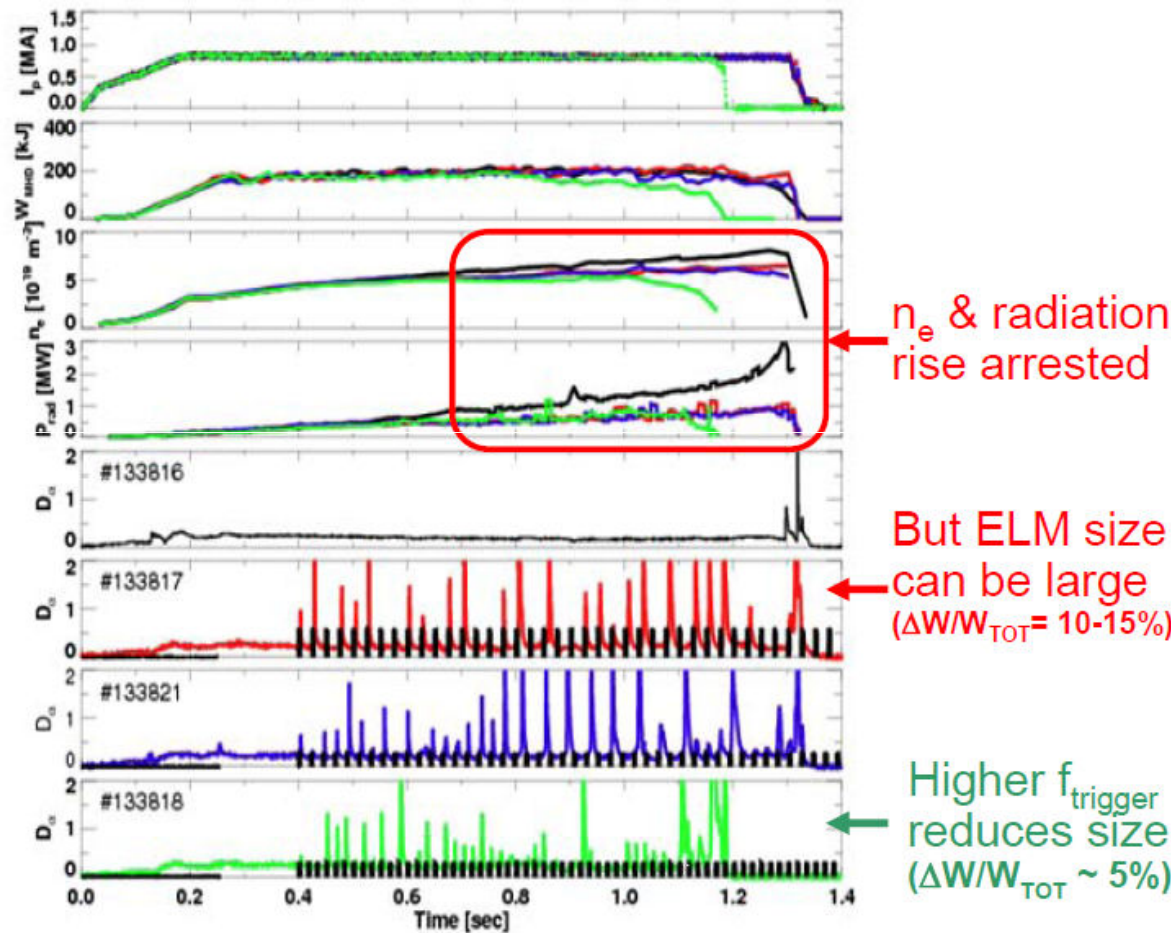


- Pre-Li, Post-Li
- Longer pulse
- Lower n_e early, higher late
- Higher stored energy
- Higher H-factor
- Higher radiated power
- ELM-free, lower recycling

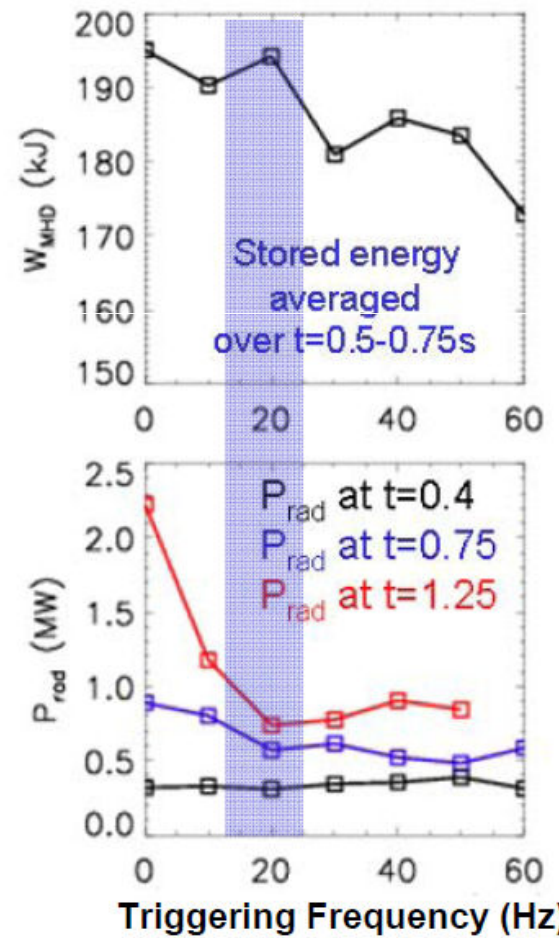
Kugel PSI08

- Now focusing on main-ion and impurity density control

ELM triggering using n=3 perturbations is being optimized to control density and radiation, maintain high confinement

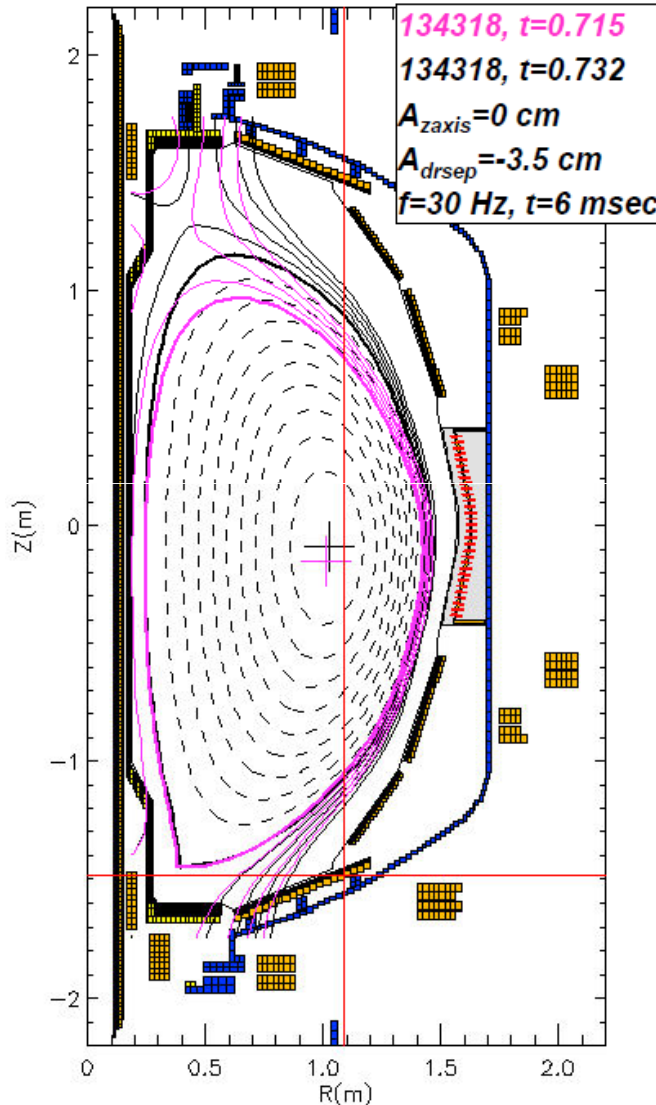


Favorable n=3 amplitude and triggering frequency found

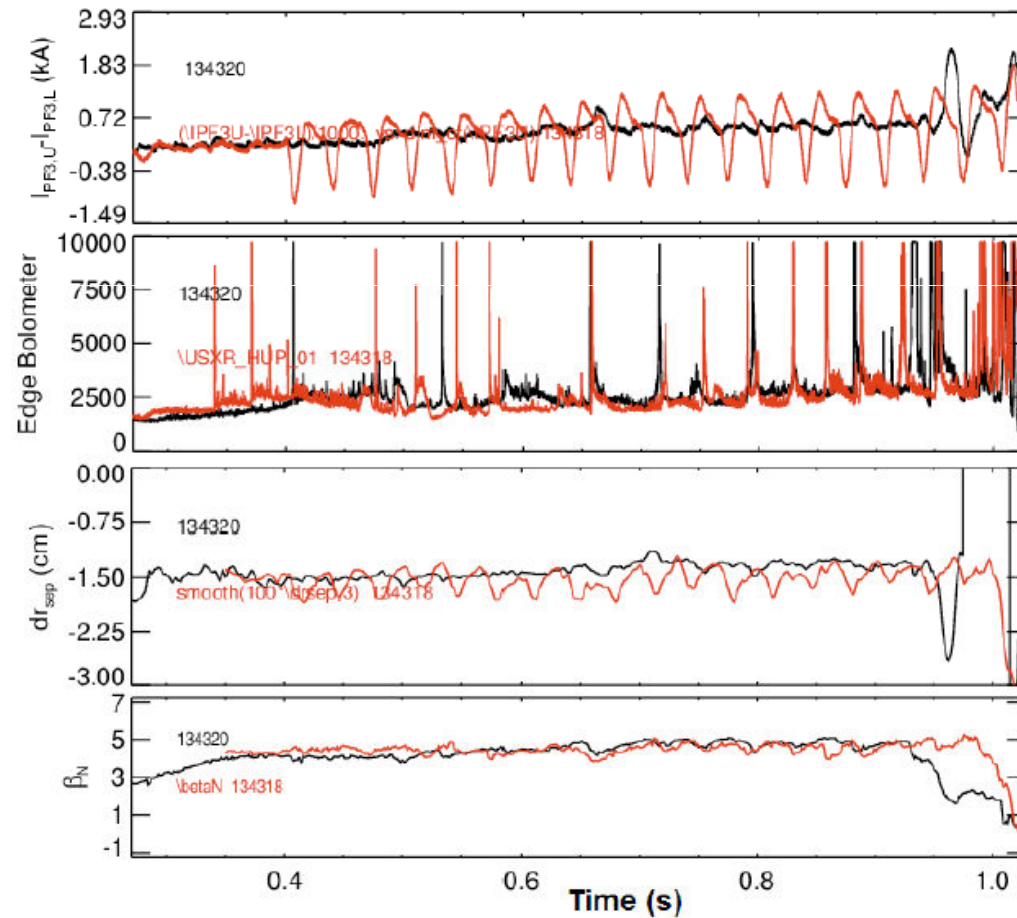


Plasma vertical position “jogs” can also trigger ELMs

(ELM triggering with jogs observed on JET, ASDEX-U, TCV)

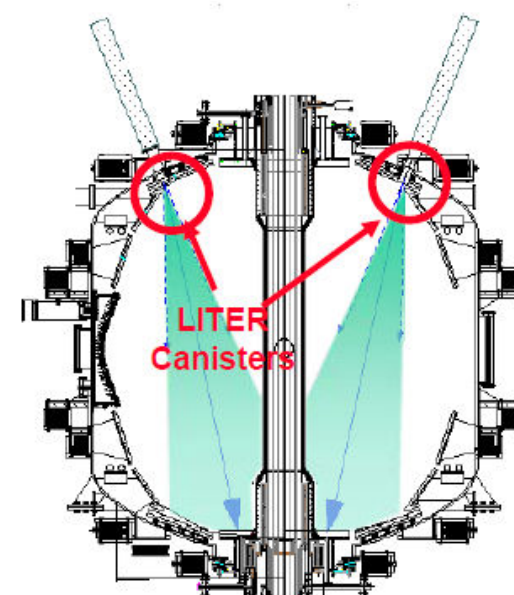
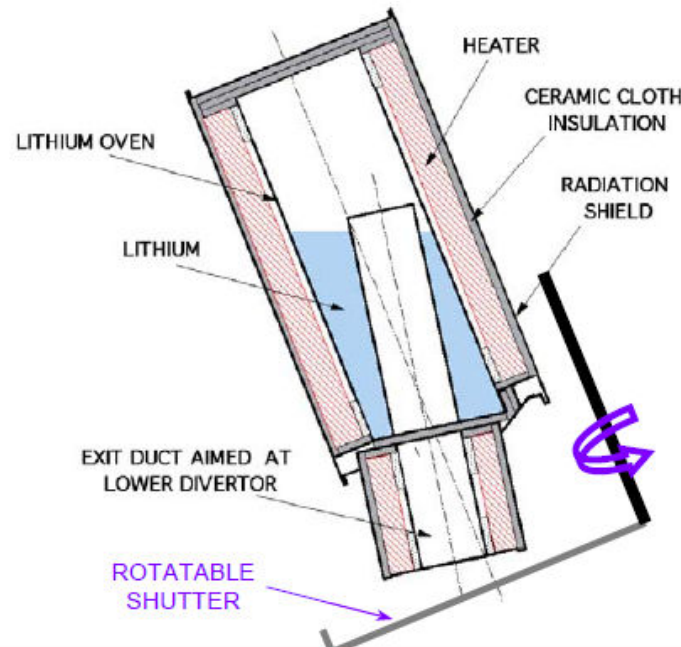


- Just beginning to explore this on NSTX...
- Thus far, triggering only works for $dr_{sep} < \sim -1\text{ cm}$



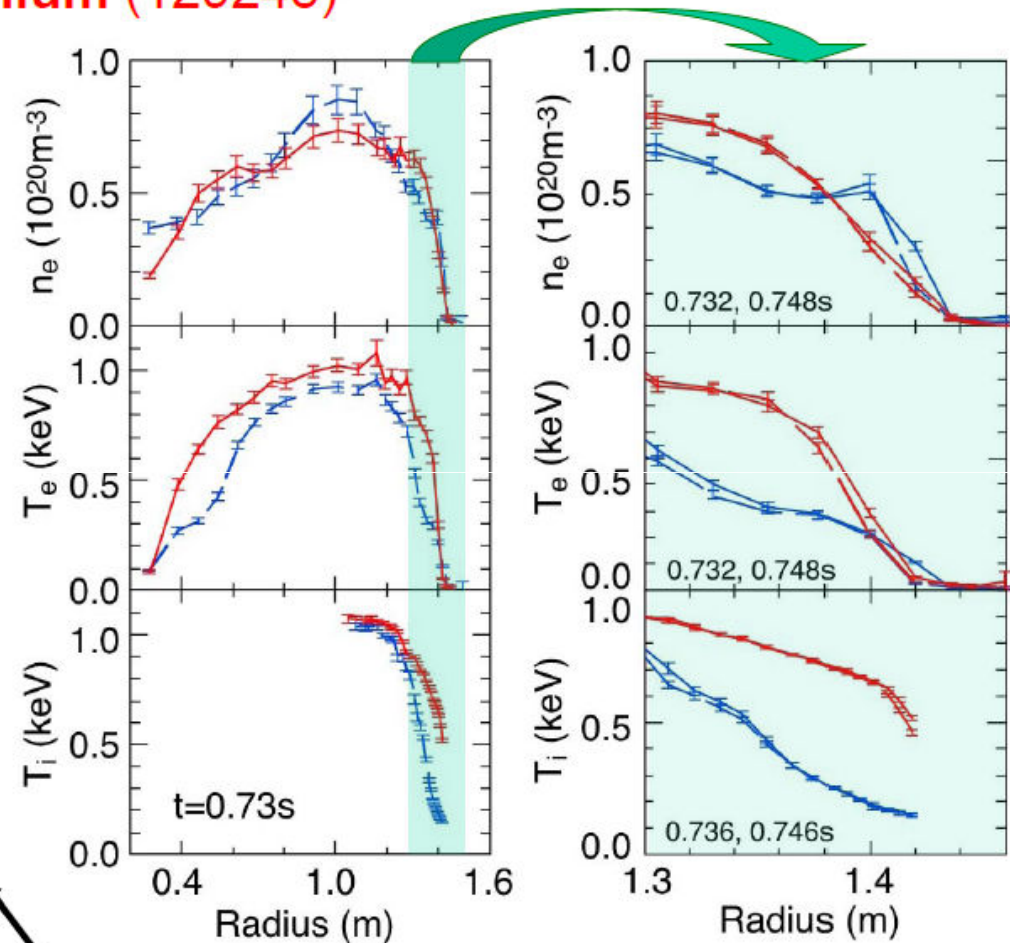
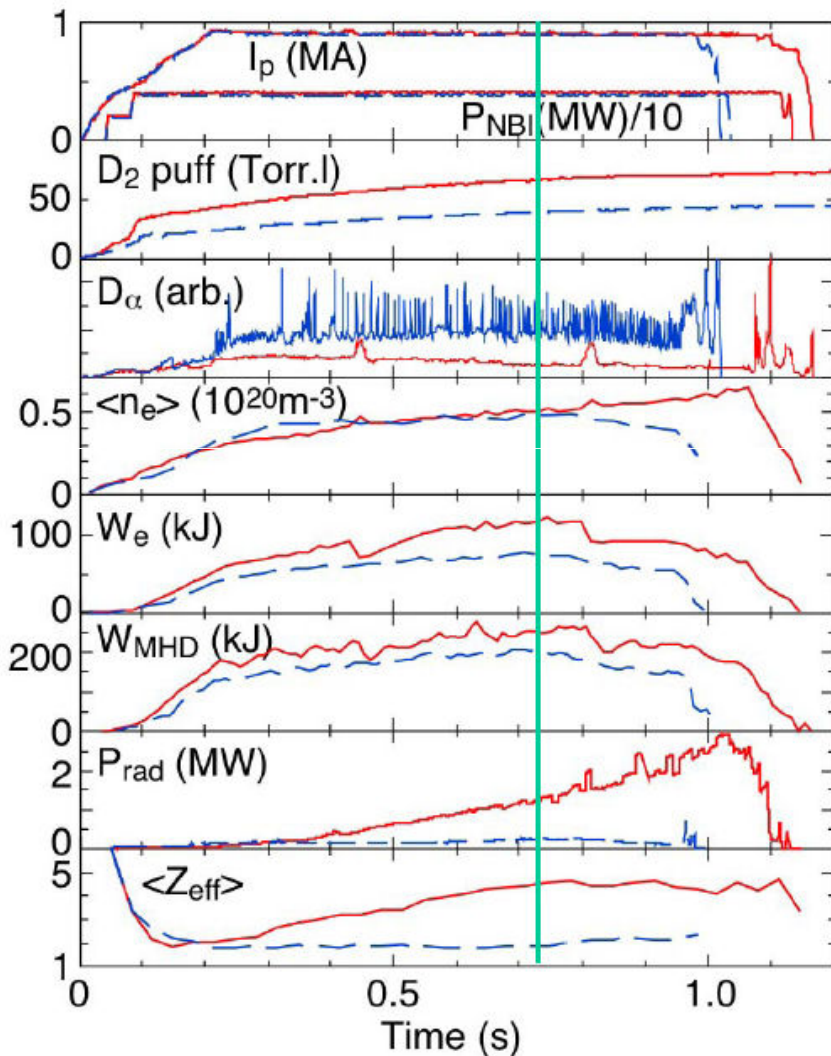
Dual LITERs Replenish Lithium Layer on Lower Divertor Between Tokamak Discharges

- Electrically-heated stainless-steel canisters with re-entrant exit ducts
- Mounted 150° apart on probes behind gaps between upper divertor plates
- Each evaporates 1 – 40 mg/min with lithium reservoir at 520 – 630°C
- Rotatable shutters interrupt lithium deposition during discharges & HeGDC
- Withdrawn behind airlocks for reloading and initial melting of lithium charge
- Reloaded LITERs 6 times during 2009 run (Mar - Aug): ~300g deposited



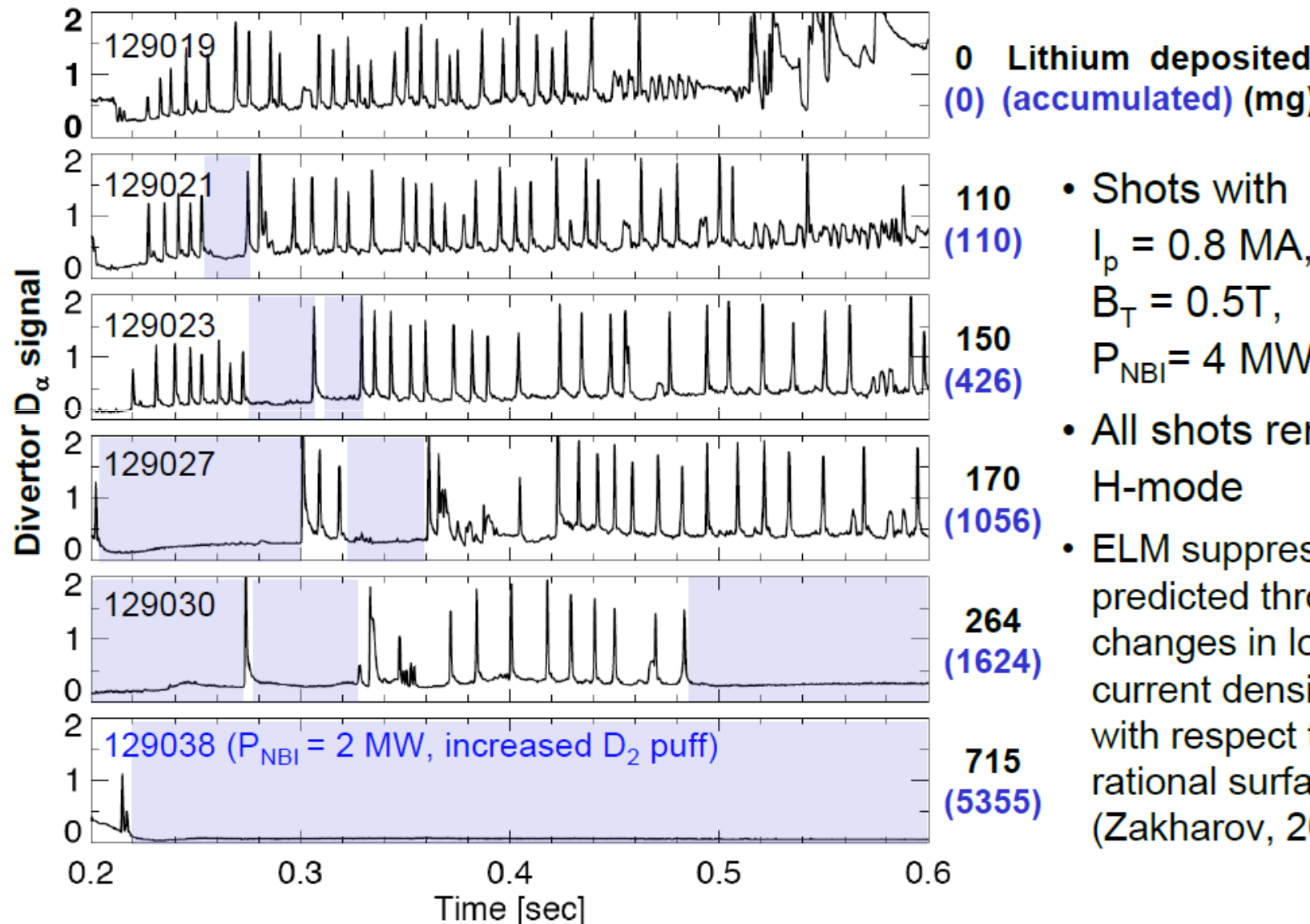
Lithium Coating Reduces Deuterium Recycling, Suppresses ELMs, Improves Confinement

No lithium (129239); 260mg lithium (129245)



Without ELMs, impurity accumulation increases radiated power and Z_{eff}

Suppression of ELMs Occurs By Lengthening and Coalescence of ELM-free Periods

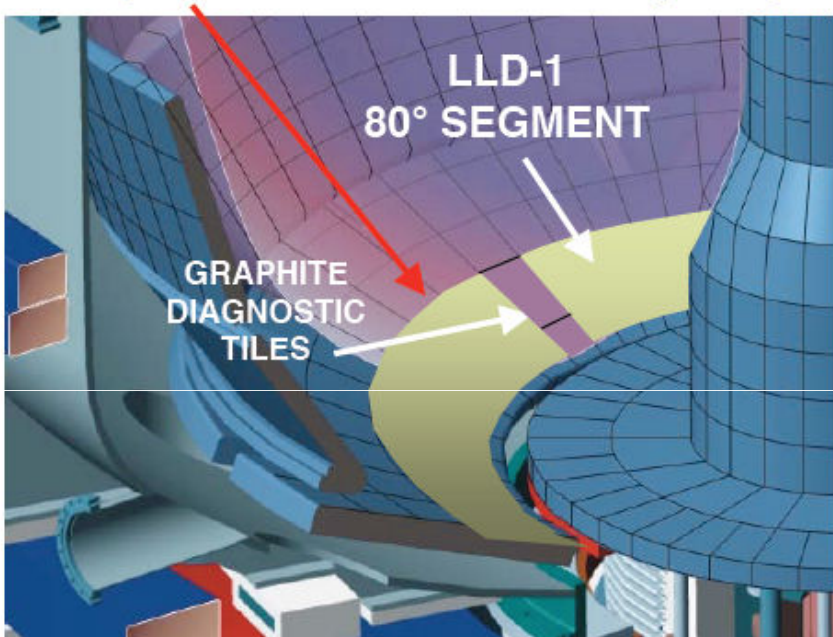


- Shots with $I_p = 0.8$ MA, $B_T = 0.5$ T, $P_{NBI} = 4$ MW
- All shots remain in H-mode
- ELM suppression was predicted through changes in location of current density gradient with respect to mode rational surfaces (Zakharov, 2006)

Liquid Lithium Divertor to Test Pumping Effectiveness

LLD Plates To Operate at Lithium Melting Temperature (200 - 400 °C)

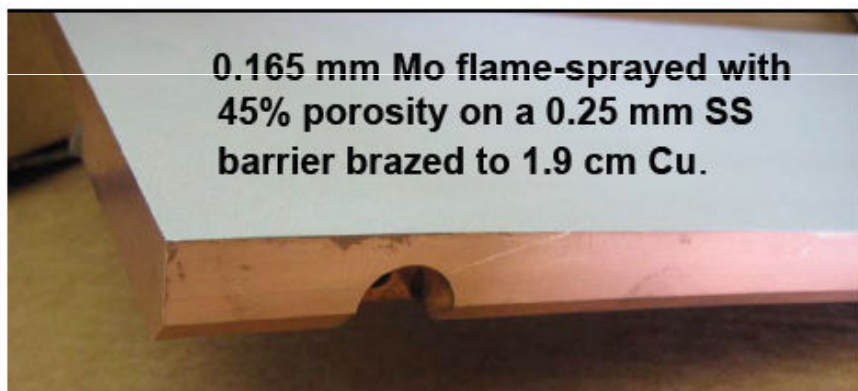
Liquid Lithium Divertor (LLD)



H. Kugel, R. Kaita (PPPL) et al.,



0.165 mm Mo flame-sprayed with
45% porosity on a 0.25 mm SS
barrier brazed to 1.9 cm Cu.



Moly-Coated LLD Plate

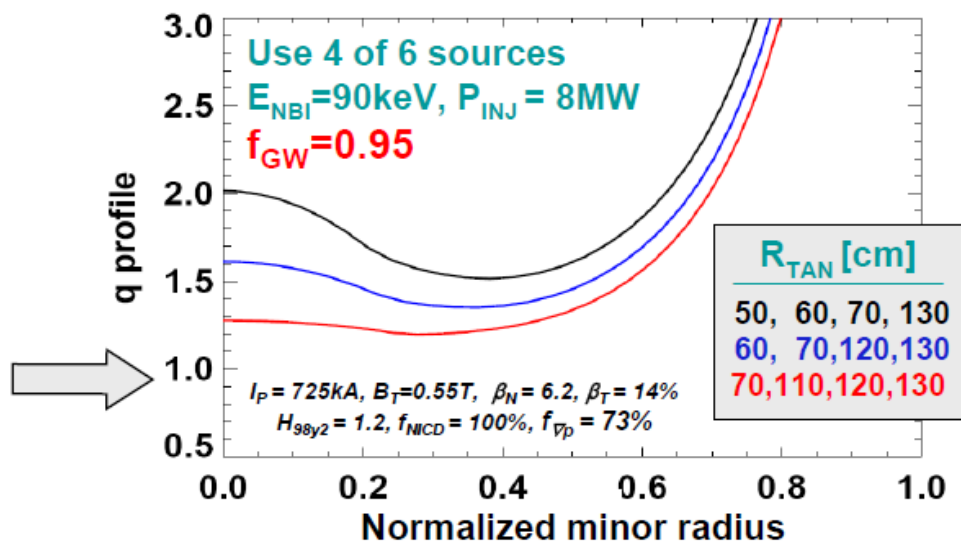
R. Nygren (Sandia NL) et al.,

- LLD installation started for FY 2010 run (completion next few weeks)
- Enhanced LLD to achieve density control - improved diagnostics and improved fill system - to be installed for FY 2011 run

Increased auxiliary heating and current drive are needed to fully exploit increased field, current, and pulse duration

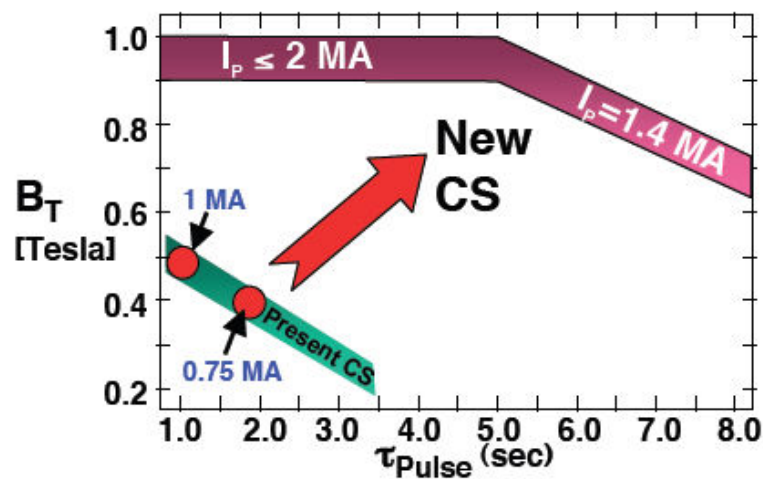
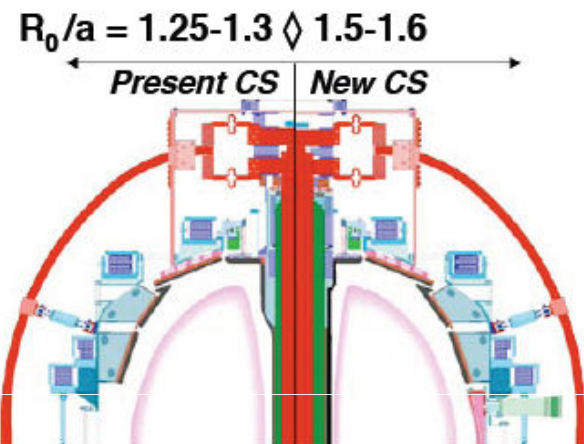
- Higher heating power to access high temperature and β at low collisionality
 - Need additional 4-10MW, depending on confinement scaling
- Increased external current drive to access and study 100% non-inductive
 - Need 0.25-0.5MA compatible with conditions of ramp-up and sustained plasmas
- Proposed upgrade: double neutral beam power + more tangential injection
 - ITER-level high-heat-flux plasma boundary physics capabilities & challenges
 - More tangential injection → up to 2 times higher efficiency, current profile control

- $q(r)$ profile very important for global stability, electron transport, Alfvénic instability behavior
 - Variation of mix of NBI tangency radii would enable core q control



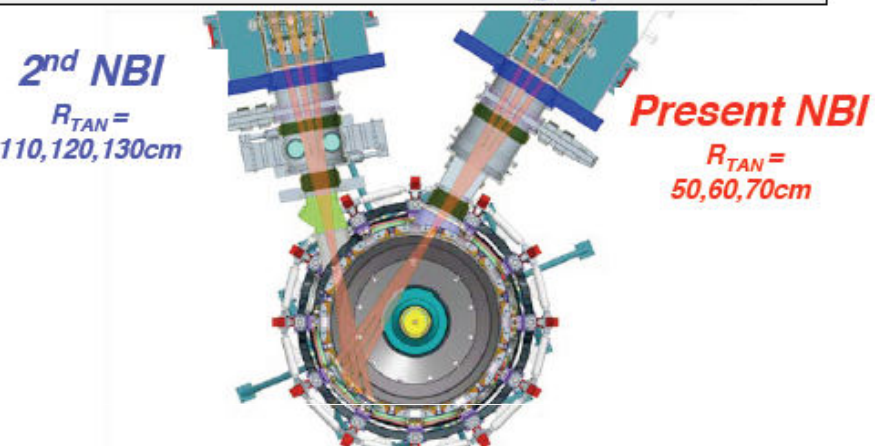
Major Facility Upgrades Planned to Bridge the Device and Performance Gap Toward Next-Step STs

New center stack for 1T, 2MA, 5s to access reduced ν^* , 100% non-inductive ST plasmas

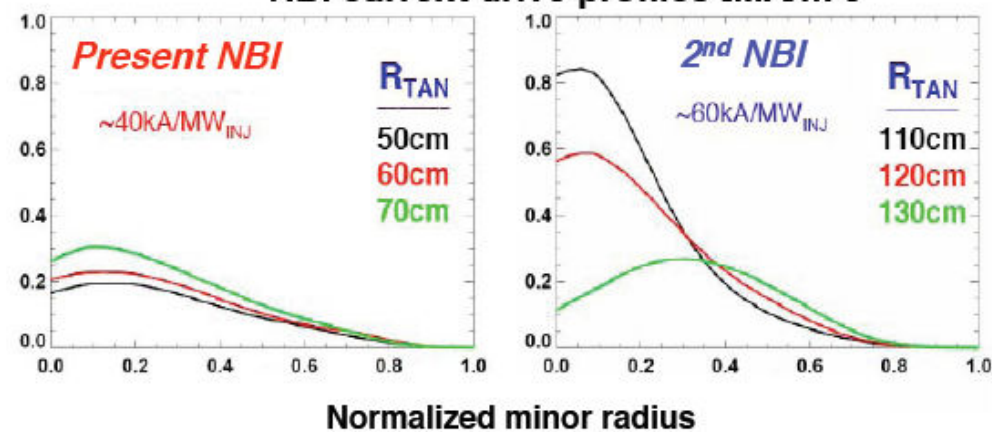


Magnet operation at ~1T (vs. 0.55T) < within a factor of 2 of next-step STs

2nd NBI with larger R_{tangency} for sustained and controllable 100% NICD + high β at low ν^*

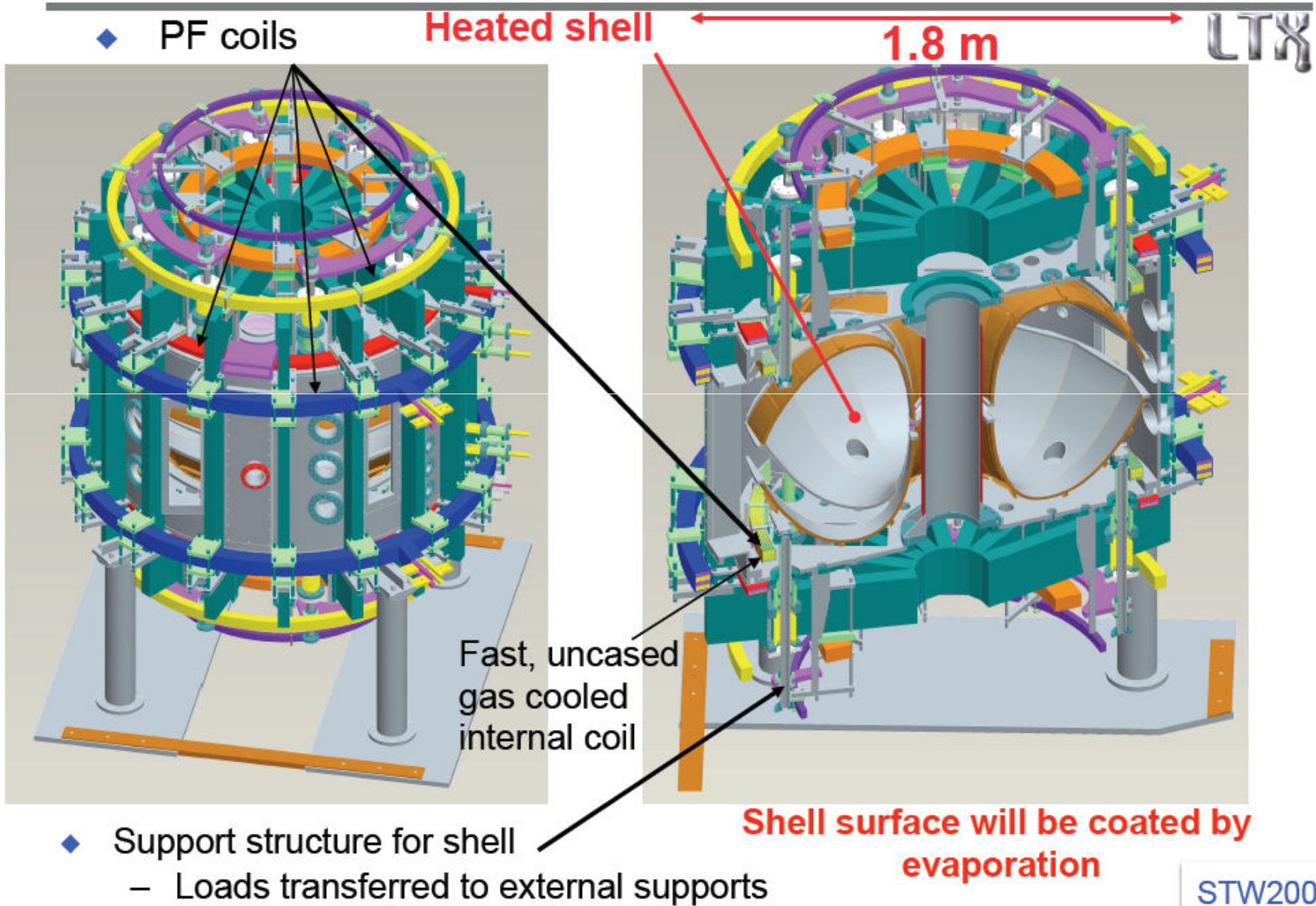


NBI current drive profiles [MA/m²]



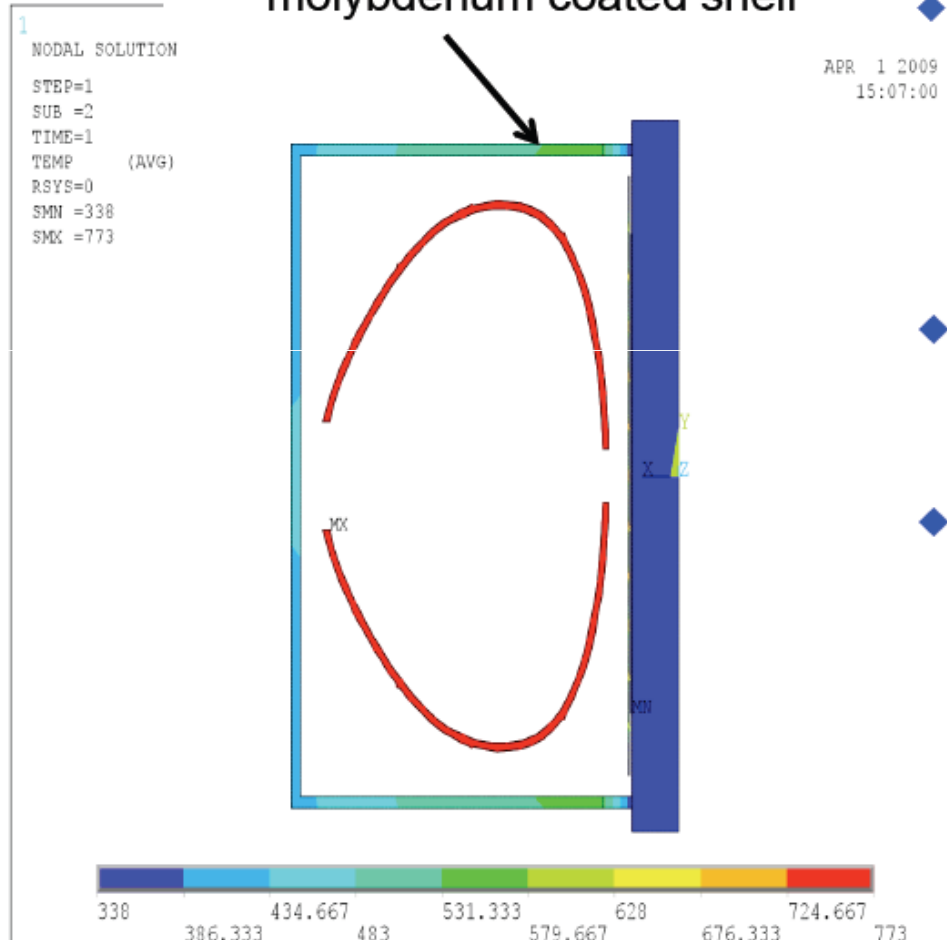
Up to 2 times higher NBI current drive efficiency, and current profile control

LTX discharges will be wall-limited on the heated, lithium-coated shell



Shell was designed for 500 °C operation to promote wetting of the SS surface by lithium

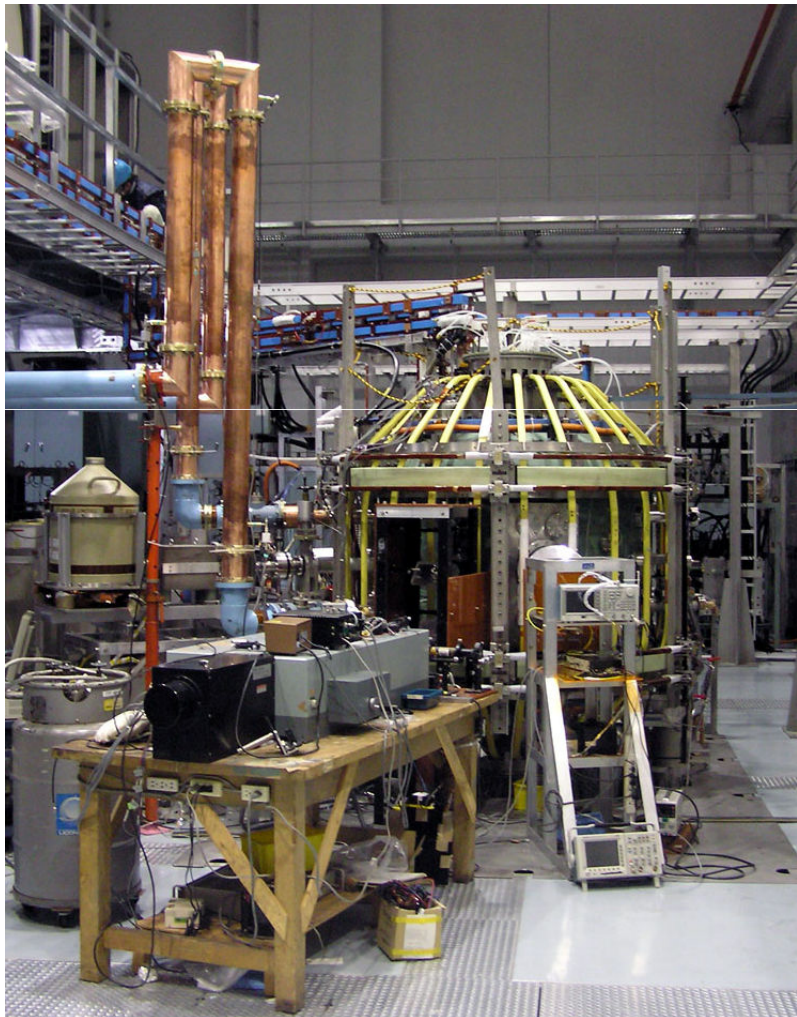
Passive heat shielding for upper, lower vessel with installation of molybdenum coated shell



- ◆ ANSYS modeling for 500 °C operation 
- ◆ Shell radiating into the vacuum chamber
 - 29 kW heater power required
 - Centerstack, vessel wall water cooled
- ◆ Centerstack is fitted with heat shield
 - Passive; polished stainless steel over silicon-bonded mica
- ◆ Shell tested to 200 °C
 - Vacuum vessel did not require water cooling; $\Delta T < 30$ °C
 - Centerstack surface $\Delta T < 2$ °C
 - Required ~10% of heater power
 - Projected continuous temperature limit: $\Rightarrow 560$ °C

TST-2 Spherical Tokamak and Heating Systems

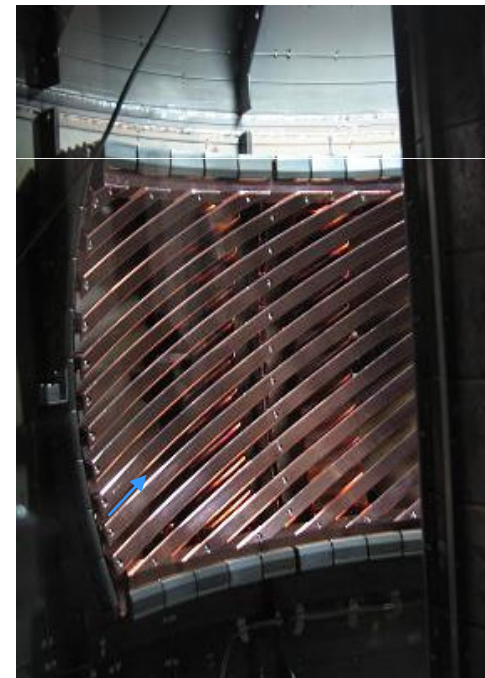
TST-2



$$\begin{aligned}R &\leq 0.38 \text{ m} \\a &\leq 0.25 \text{ m} \\B_\phi &\leq 0.3 \text{ T} \\I_p &\leq 0.2 \text{ MA}\end{aligned}$$

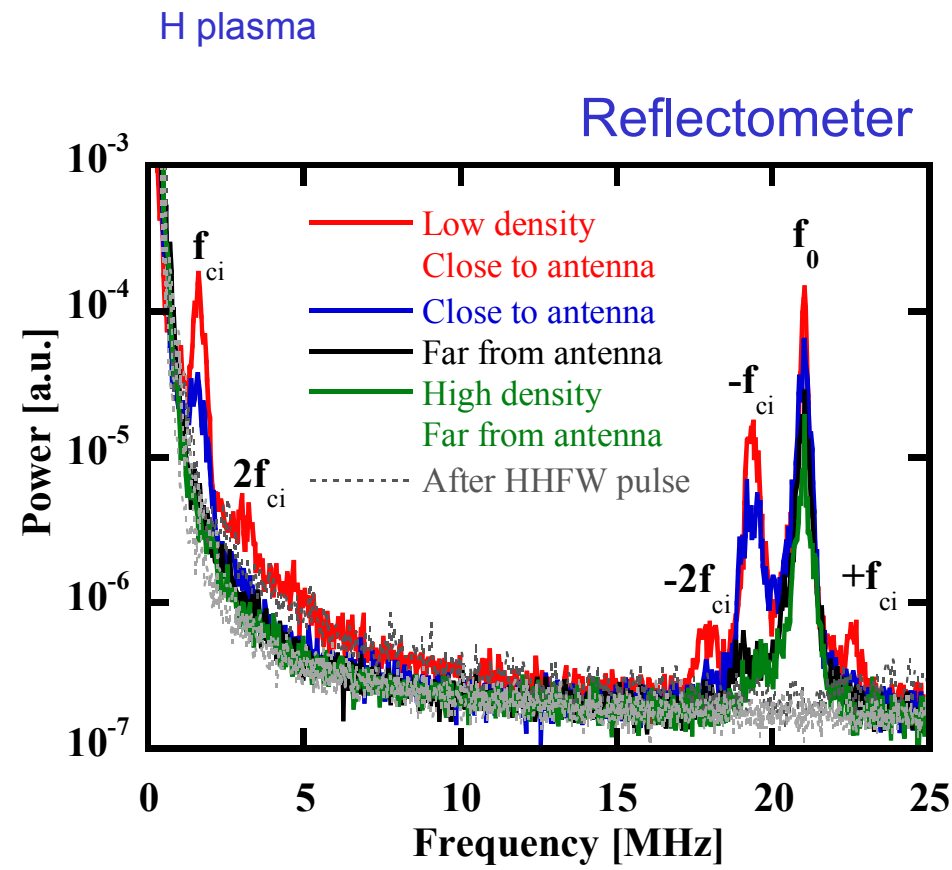
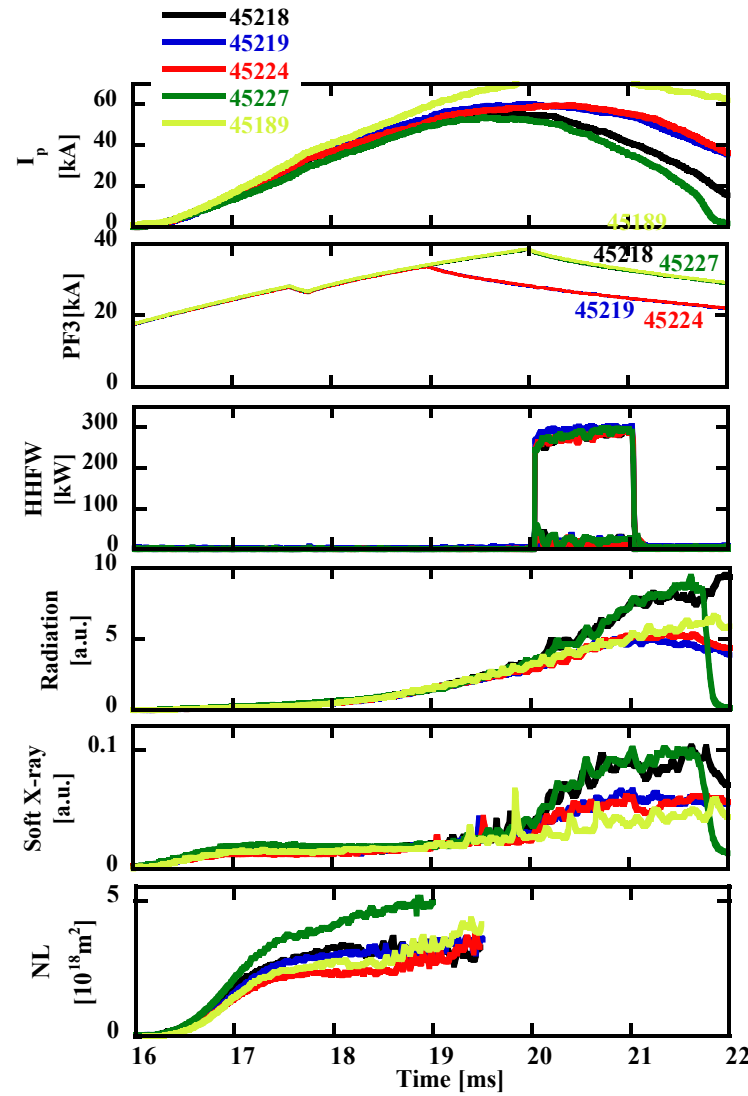
2-Strap HHFW Antenna
(only 1 strap was used)

21MHz, up to 400 kW
(up to 30 kW was used)

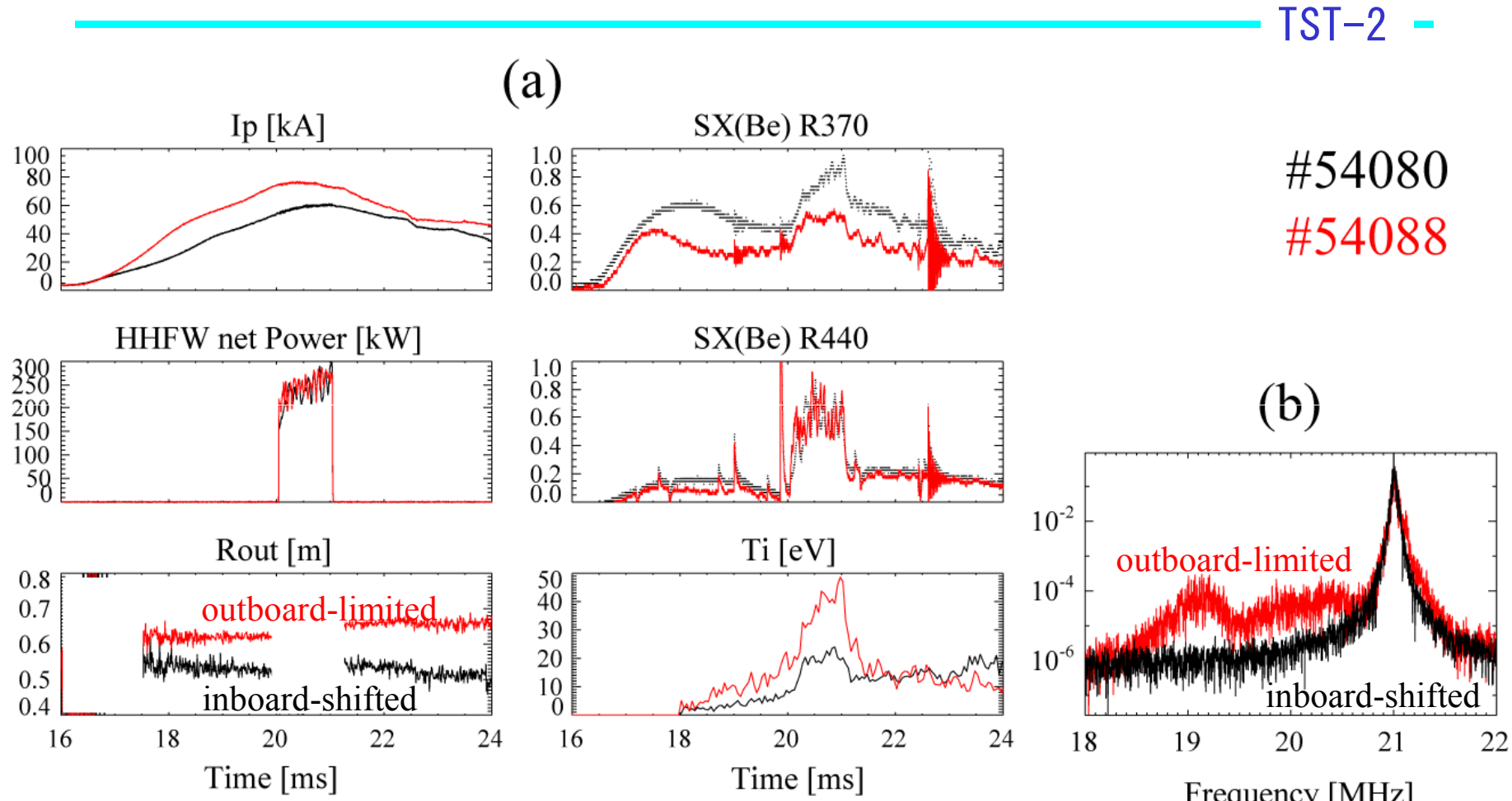


X-mode launch horn antenna for ECH
2.45 GHz, up to 5 kW

PDI Spectra Measured by Reflectometer

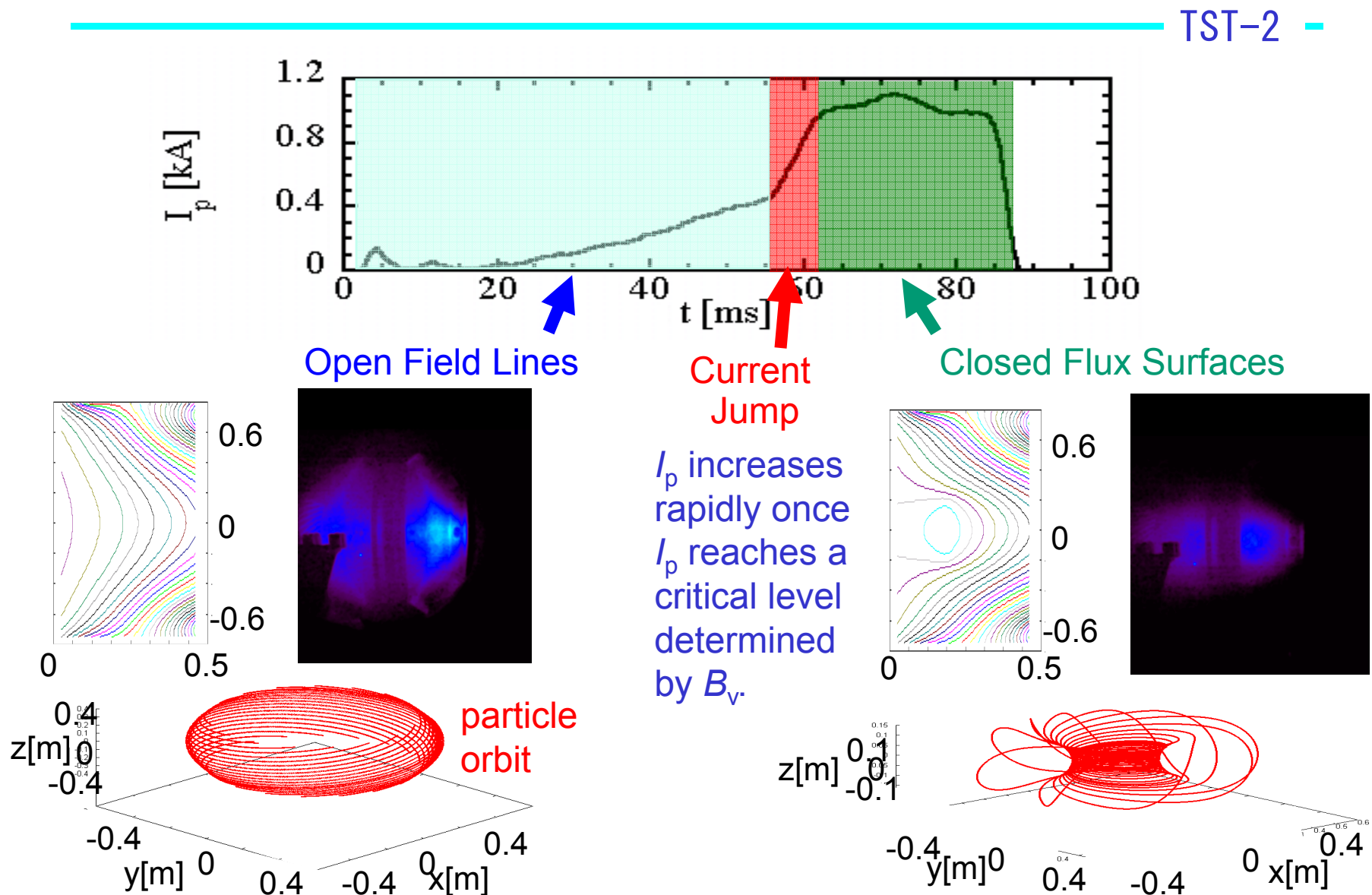


Correlation Between PDI and Electron/Ion Heating

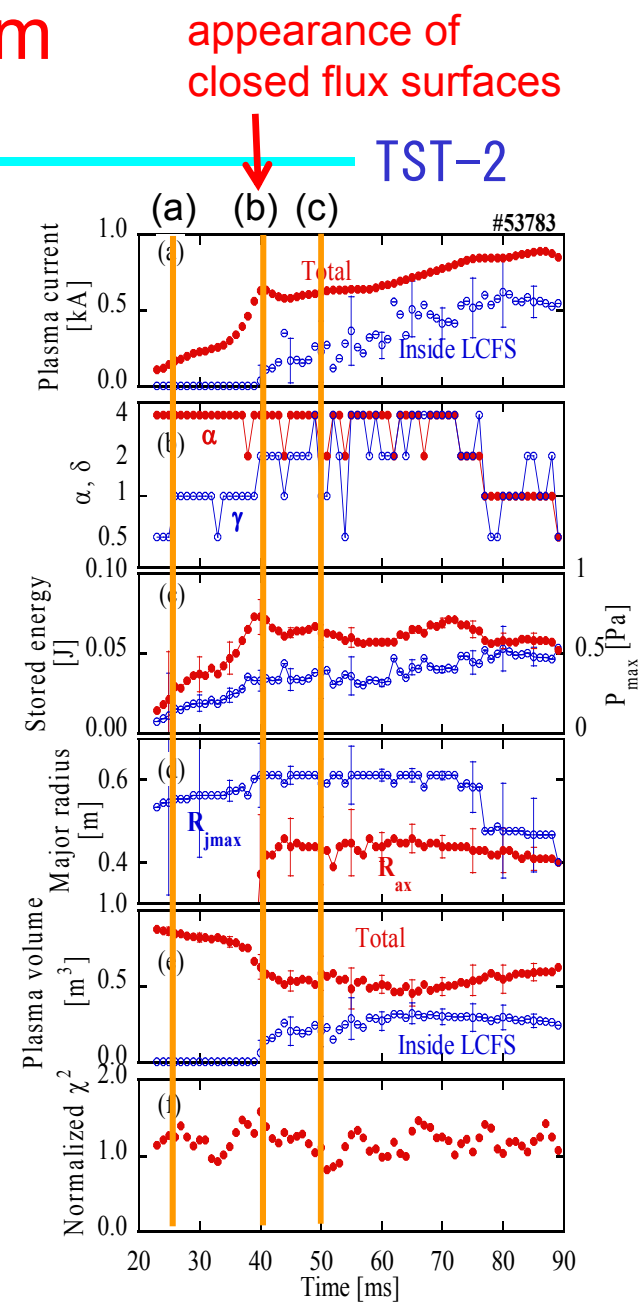
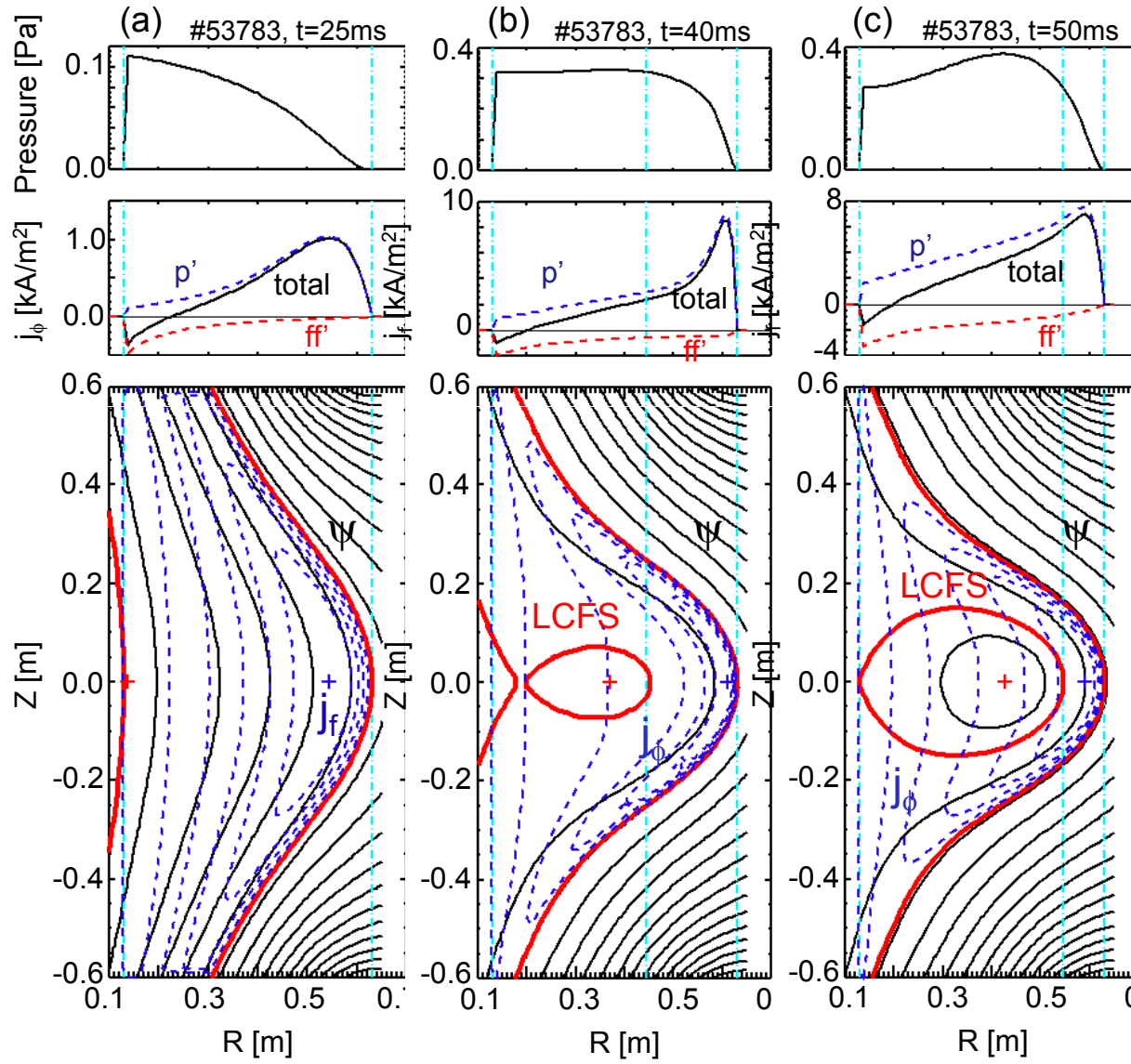


Stronger PDI \leftrightarrow • Less electron heating
• More ion heating

3 Phases of I_p Start-up by ECH



Evolution of Equilibrium

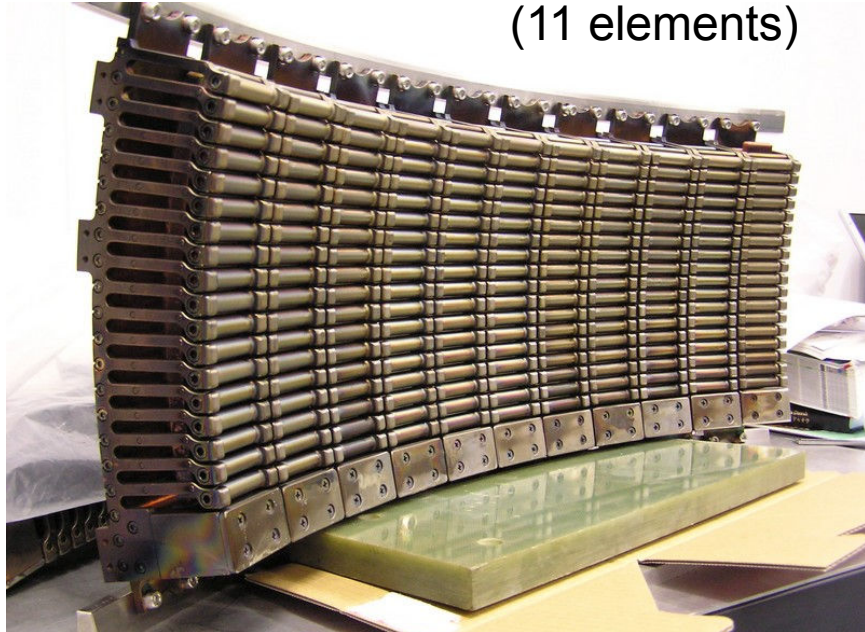


Preparation for LHCD Experiment

TST-2 -

200 MHz transmitters
(200 kW x 4, from JFT-2M)

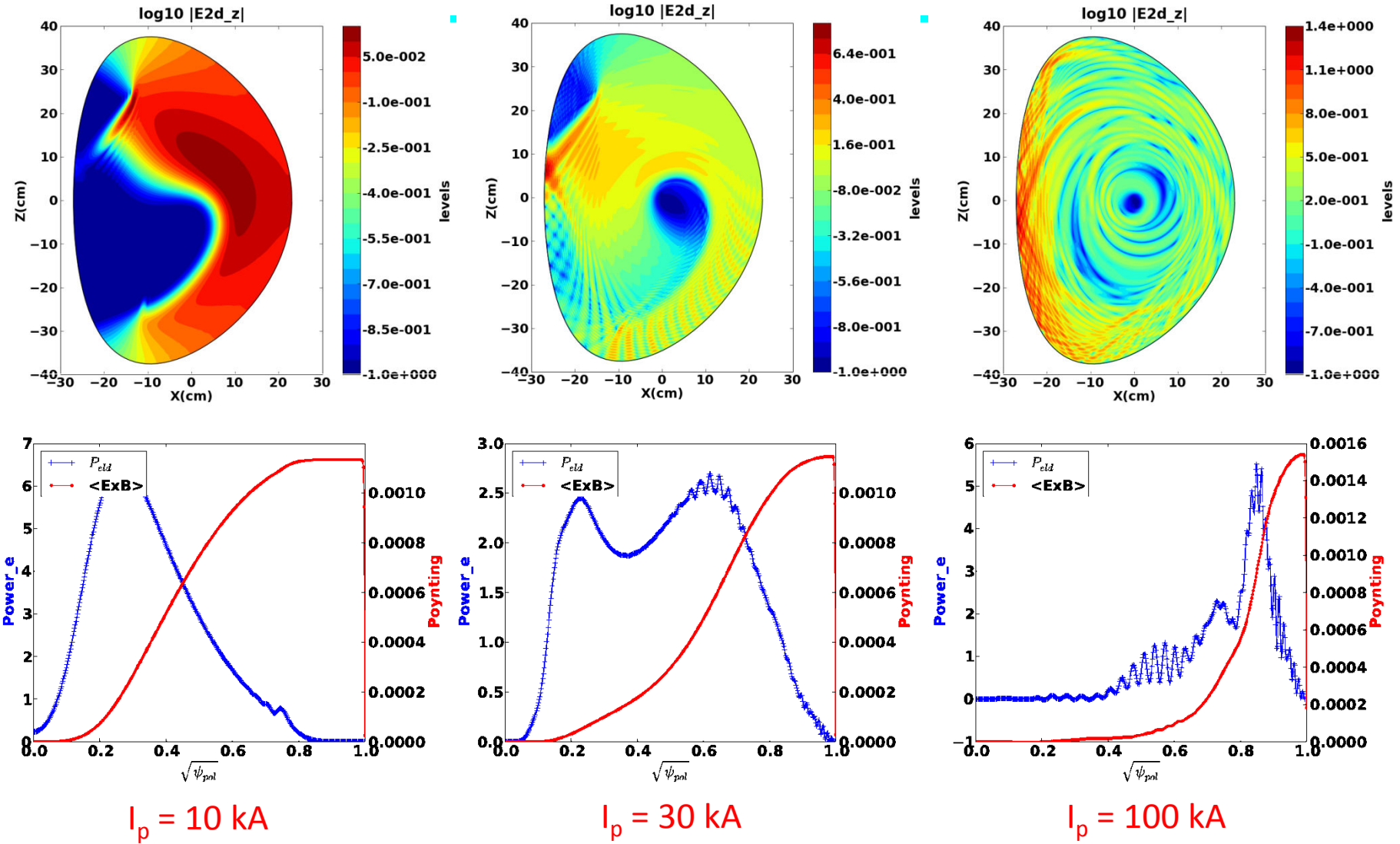
Combine antenna
(11 elements)



- Initially, the combine antenna used on JFT-2M, adapted for use on TST-2, will be used to excite a unidirectional fast wave with $n_\phi = 12$ (corresponding to $n_{||} = 5$).
- Direct excitation of the LH wave is planned in the future.
- The fast wave can mode convert to the LH wave and drive current.

I_p scan at low n_e

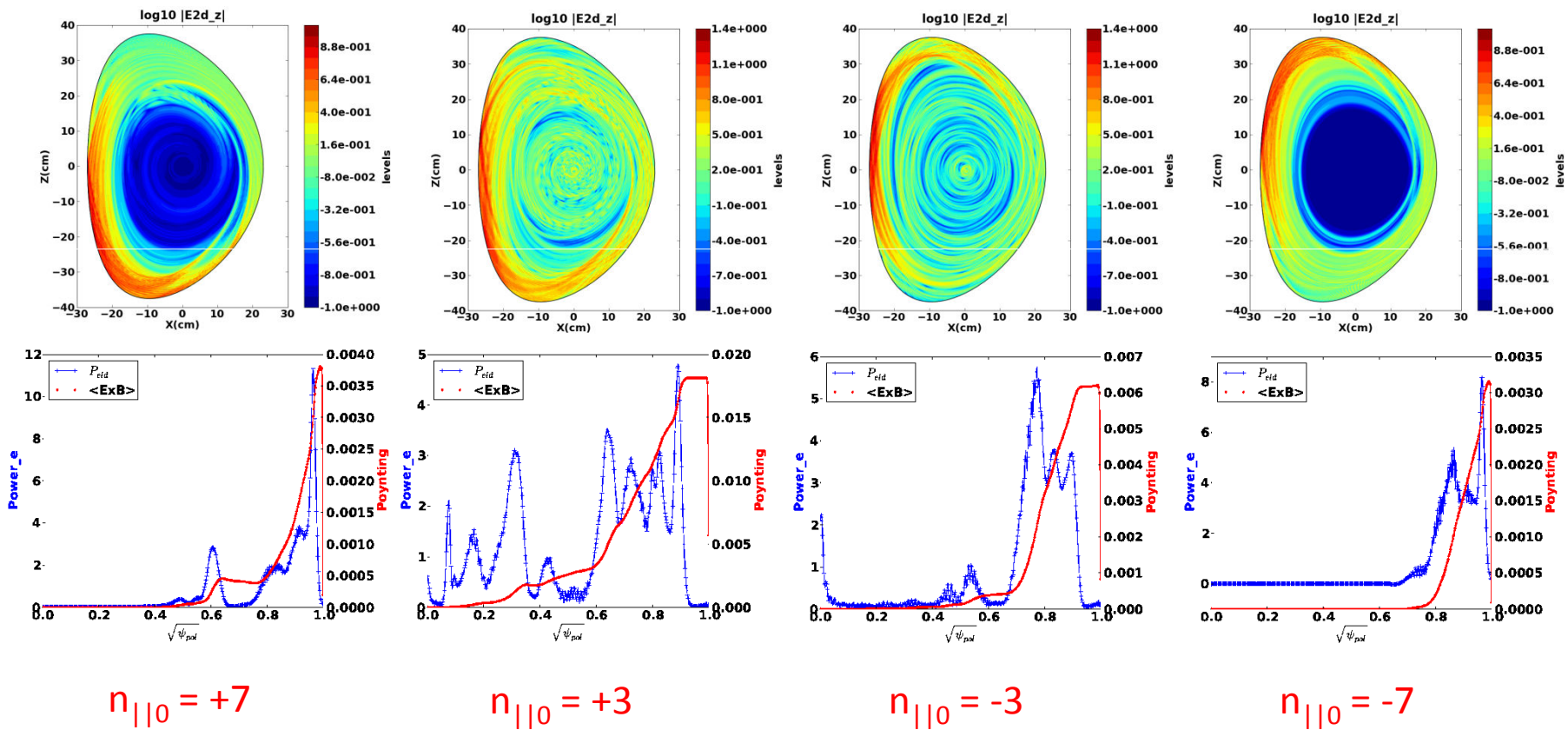
$$n_{e0} = 1 \times 10^{17} \text{ m}^{-3}; T_{e0} = 1 \text{ keV}; n_{||0} = 7; \theta_{\text{ant}} = 0^\circ$$



Core absorption expected only at very low n_e ($< 5 \times 10^{18} \text{ m}^{-3}$) and I_p ($< 50 \text{ kA}$).

$n_{\parallel 0}$ scan at high I_p

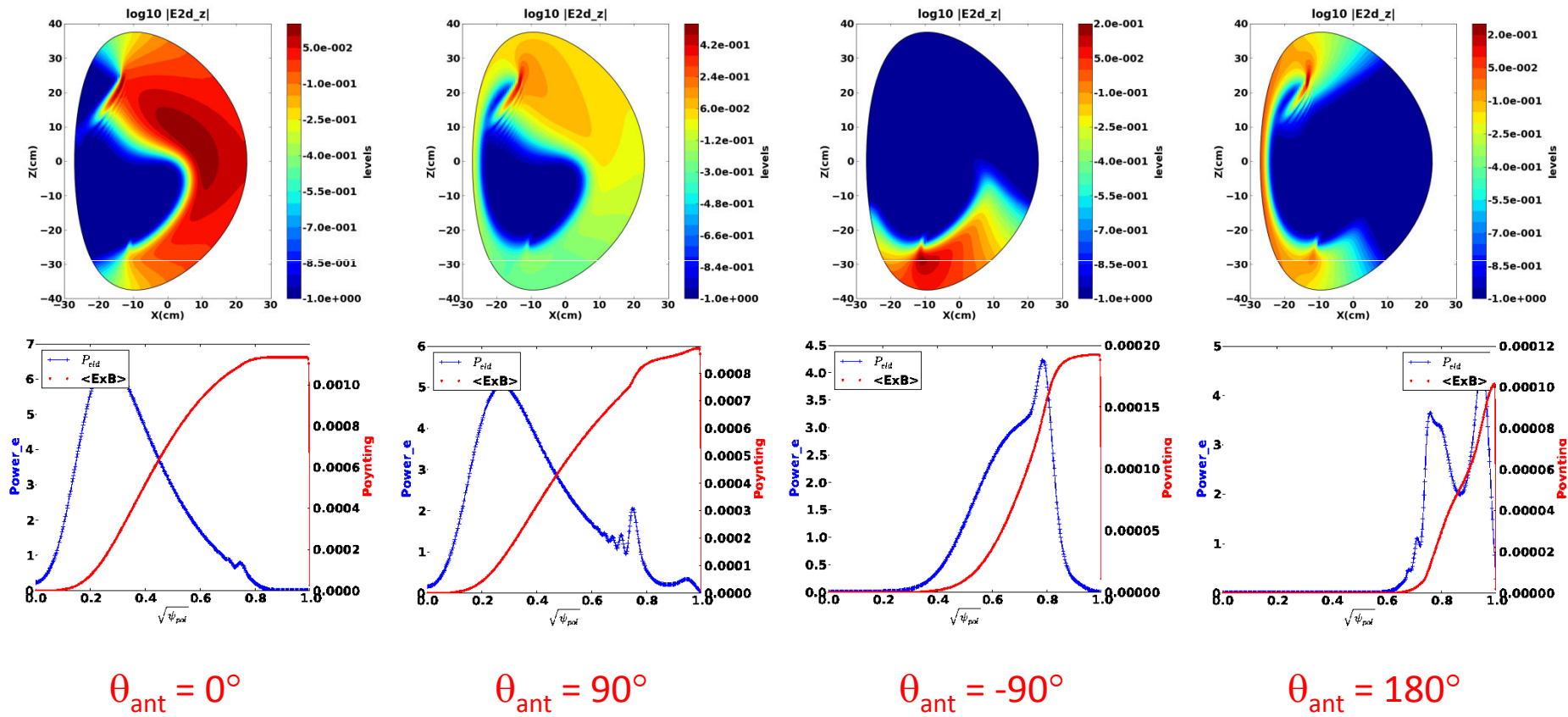
$$n_{e0} = 1 \times 10^{18} \text{ m}^{-3}; T_{e0} = 1 \text{ keV}; I_p = 100 \text{ kA}; \theta_{\text{ant}} = 0^\circ$$



At high plasma current (100 kA) only low n_{\parallel} LHW can reach the plasma core.

Antenna location scan

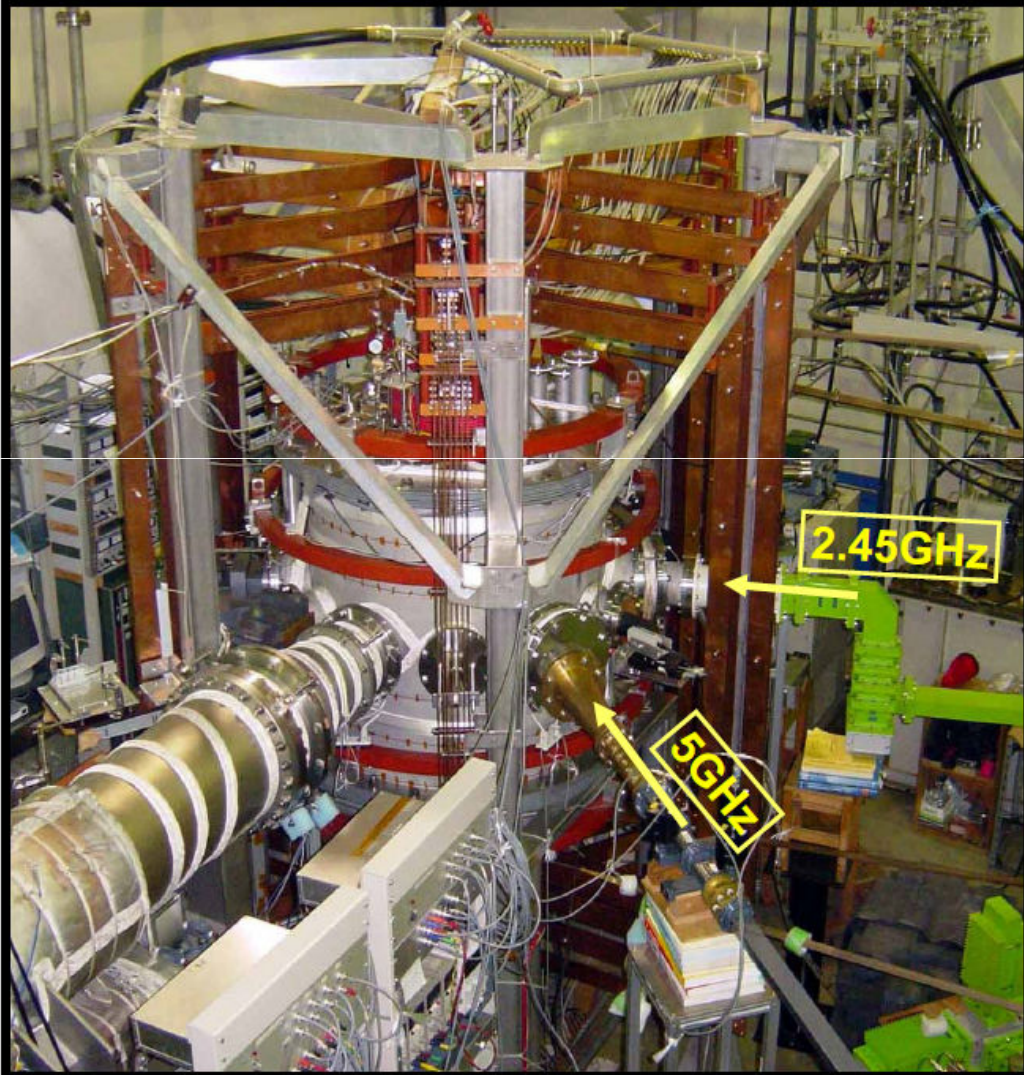
$$n_{e0} = 1 \times 10^{17} \text{ m}^{-3}; T_{e0} = 1 \text{ keV}; I_p = 10 \text{ kA}; n_{||0} = 7$$



Wave excitation from the low field side midplane is adequate.



Low Aspect ratio Torus Experiment (LATE) is exploring non-solenoidal start-up by ECH/ECCD



Device Parameters:

Vacuum vessel :

diameter = height = 1m

Center post : diam. = 11.4 cm

Toroidal coils :

$B_t = 0.48 \text{ kG}$ ($R=25\text{cm}$), 10 s

$B_t = 1.15 \text{ kG}$ ($R=25\text{cm}$), 0.3 s

Vertical coils: 3 sets

Vertical position control

Microwaves:

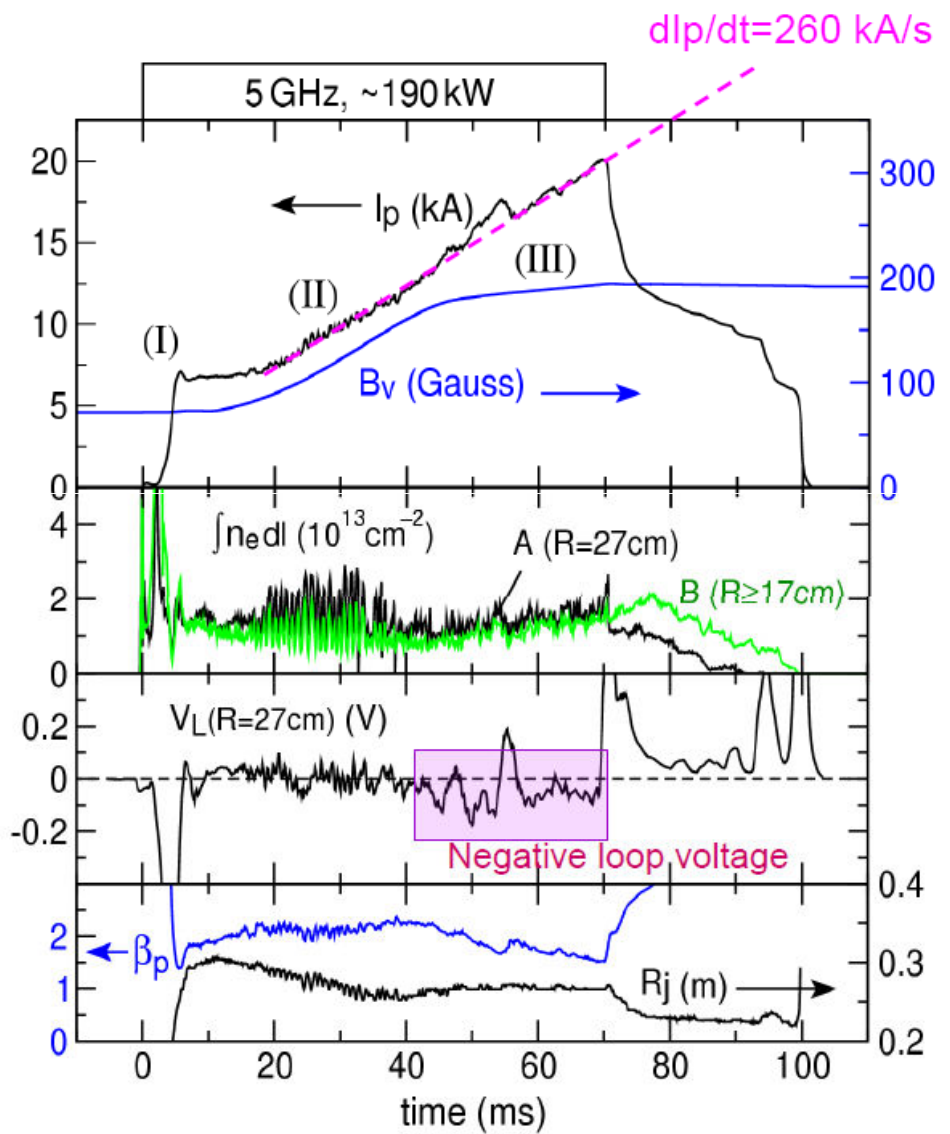
2.45 GHz 5kW CW x 2,
20kW 2s x 2

5.0 GHz 200kW 0.07s

Diagnostics:

Magnetics (17 Flux loops),
70GHz interferometer (3 chords),
SX cameras (4-poloidal, 1-toroidal), X-ray PHA (CdTe),
Fast visible camera,
Langmuir probes, Spectrometer

Current ramps rapidly up to 20kA by 5 GHz EC power and Bv control



Discharge evolves in three stages

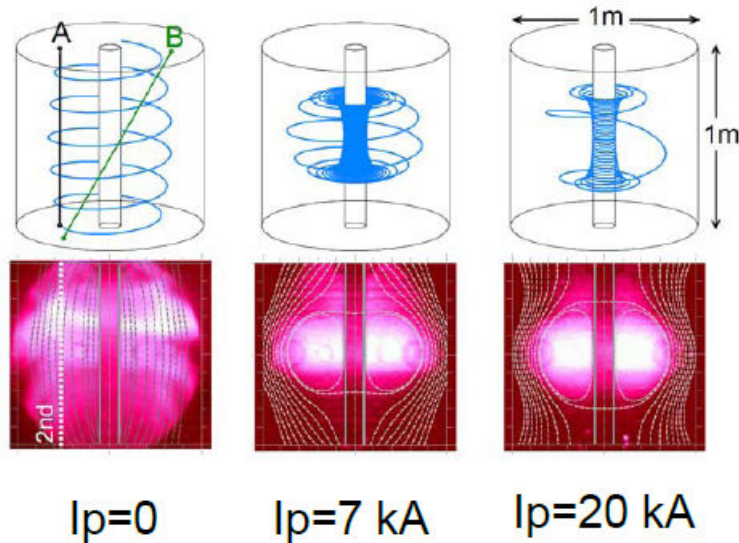
- I Closed surface is formed under steady B_v
- II I_p ramps up with a ramp of B_v
- III B_v -ramp is turned very slow. I_p still ramps up.

\Rightarrow Negative loop voltage $V_L \sim -0.1 \text{ V}$

$\beta_p \sim 1.5$ due to tail

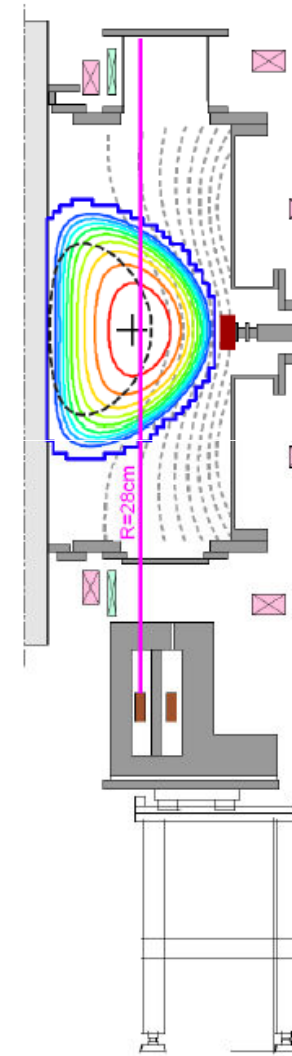
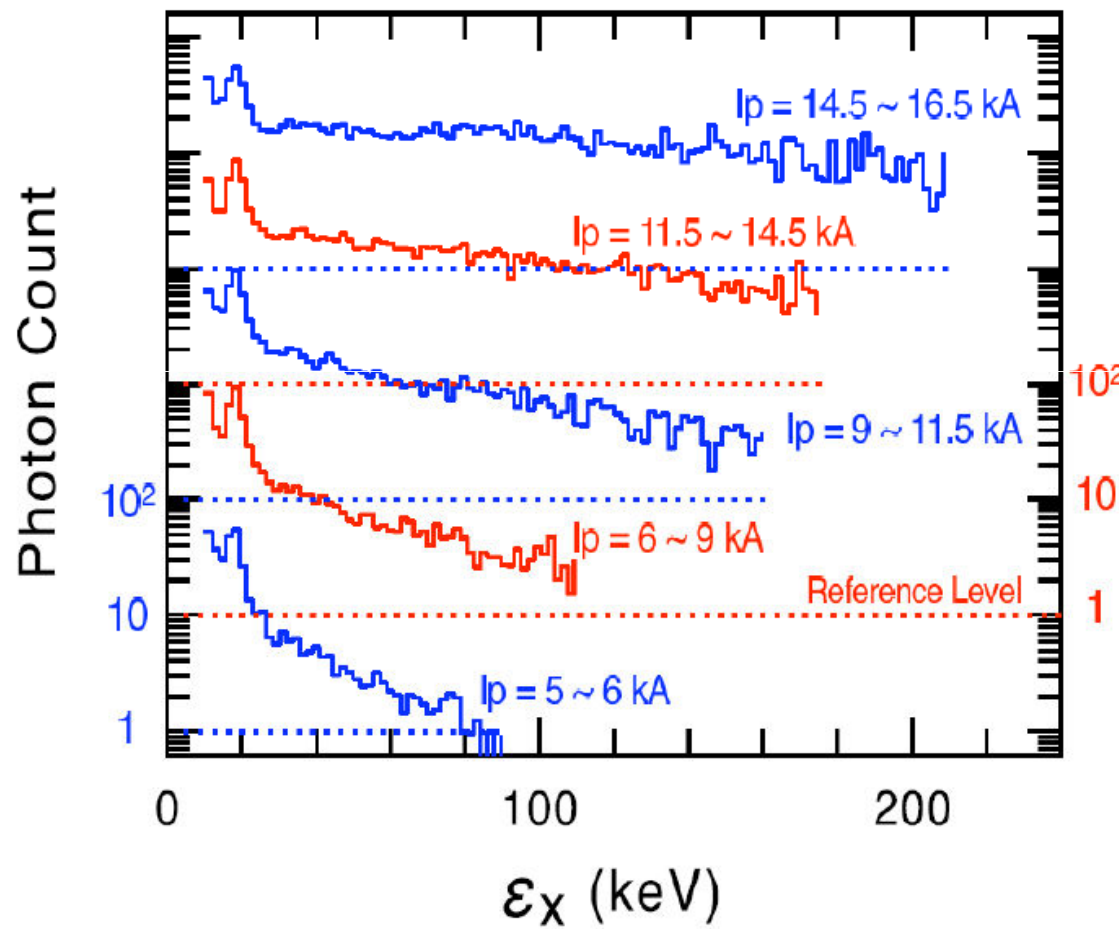
(β_p -thermal < 0.05) when $I_p = 20 \text{ kA}$

\Rightarrow Fast electron tail energy $\sim 100 \text{ keV}$

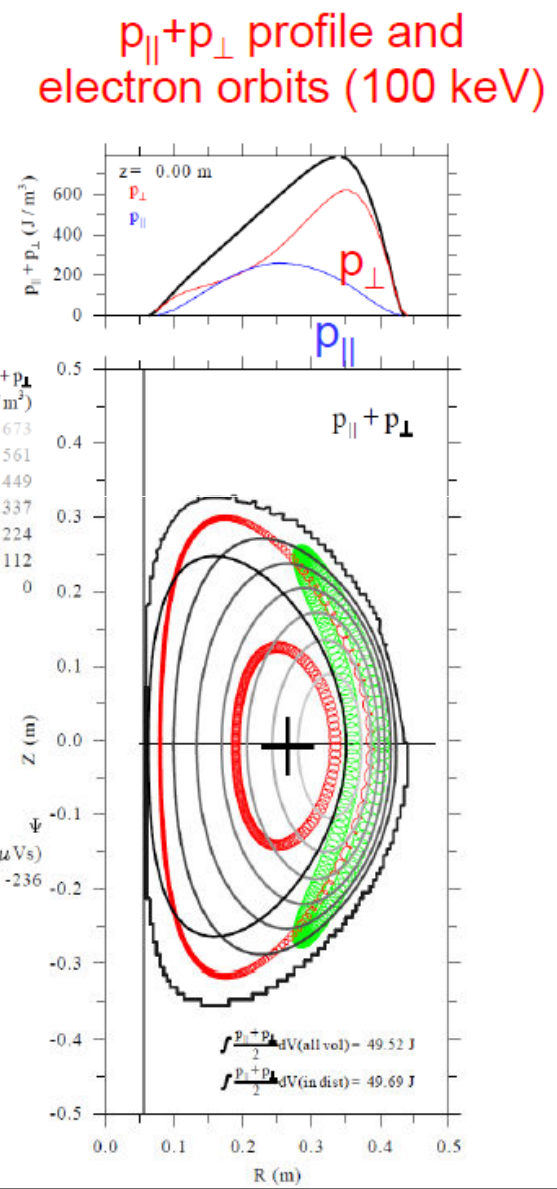
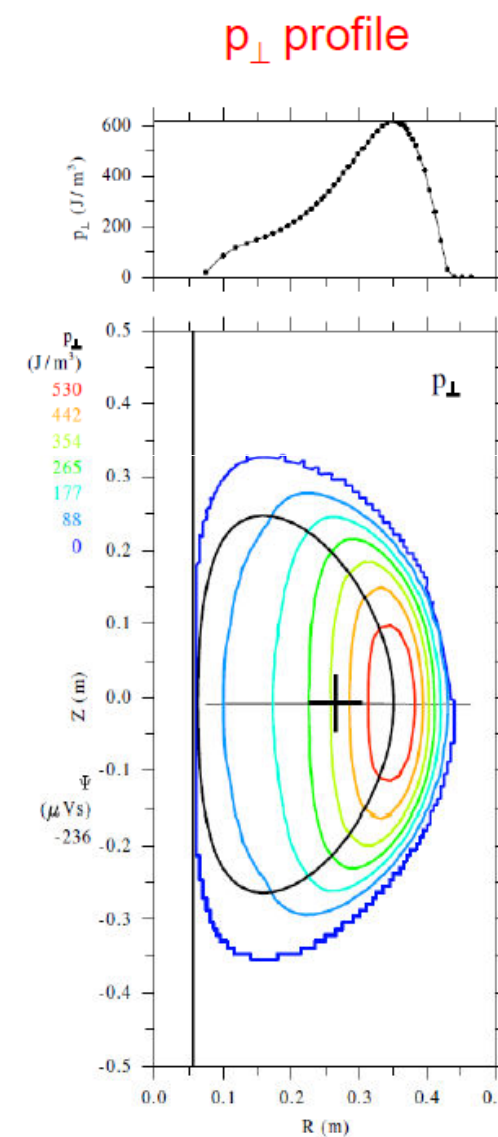
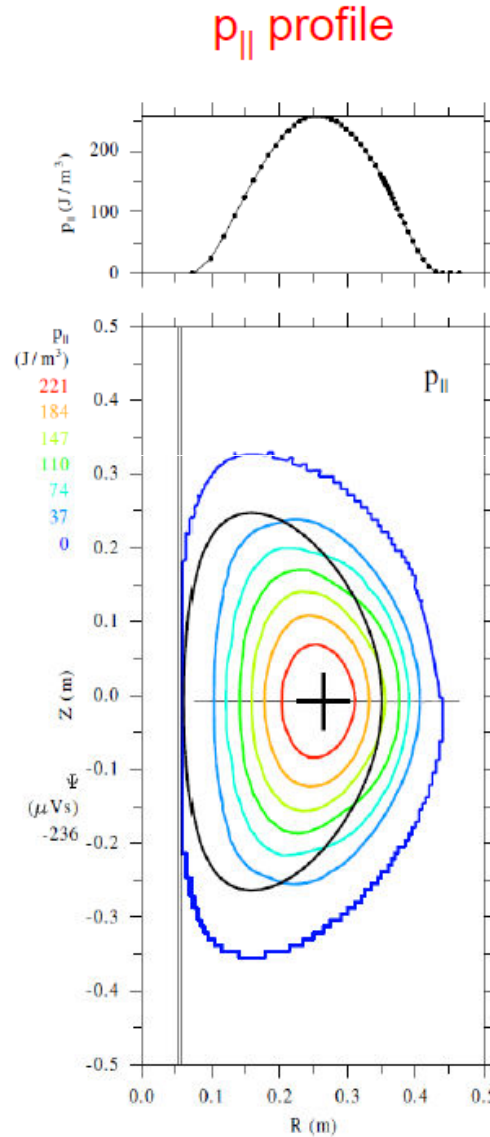




Hard X-ray energy range evolves as I_p ramps up.

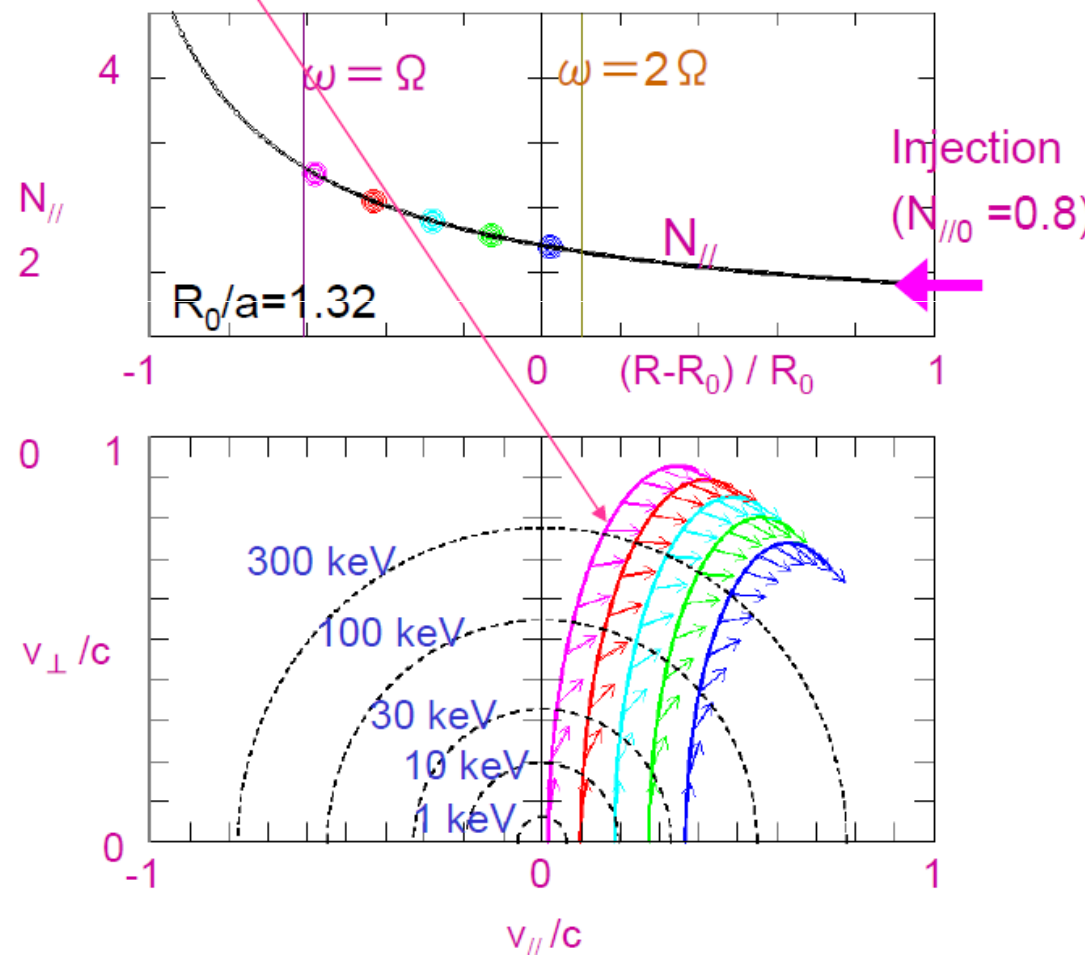


Equilibrium Pressure Profiles (p_{\parallel} , p_{\perp}) deduced by anisotropic pressure model for the 20 kA plasma



In the stage III, high N_{\parallel} EB waves overdrive electrons from the thermal tail towards the energetic range well beyond the runaway velocity against the counter Electric force.

EC resonance ellipses for high N_{\parallel} Electron Bernstein Waves
 (Arrows denote the direction of quasi-linear diffusion)



$$N_{\parallel} = \frac{\mathbf{N} \cdot \mathbf{B}}{B} = \frac{N_{\phi}B_{\phi} + N_P B_P}{B}$$

$$\cong N_{\phi} + \frac{N_P B_P}{B}$$

$$N_{\phi} = \frac{N_{\phi 0} R_0}{R}$$

Toroidal wave length decreases as $\propto R$. Then N_{\parallel} increases as $\propto 1/R$, significant in the low aspect ratio plasma.

Wave force that pushes resonance electrons parallel to the magnetic field is proportional to N_{\parallel} .

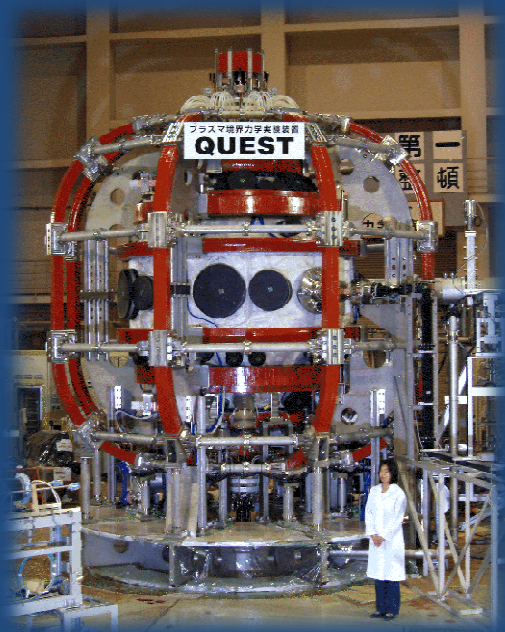
Electromagnetic waves (O and X modes) can not have high N_{\parallel} .

EB waves are an electrostatic mode and can have high N_{\parallel} .

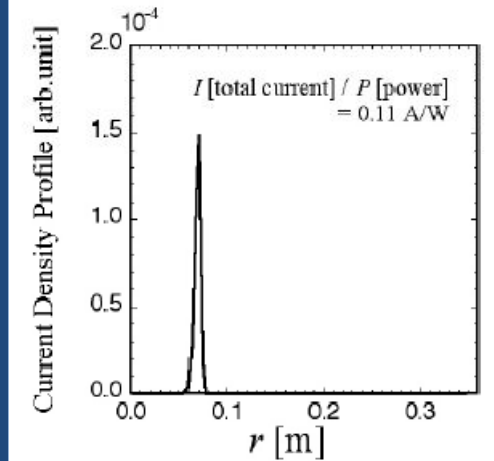
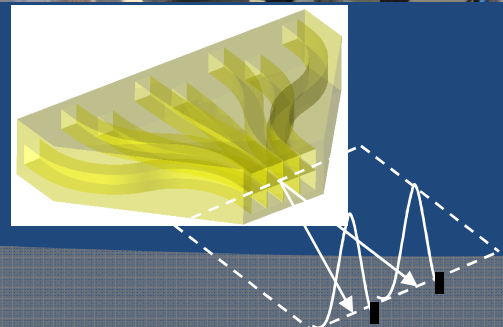
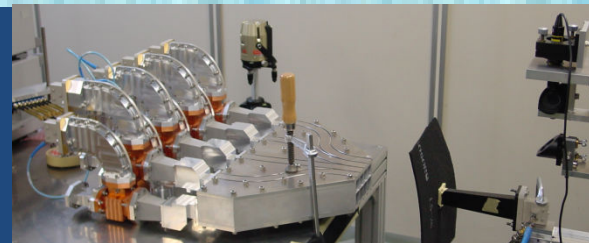
QUEST Experiment

R=0.68m
a=0.4m
A=1.78
 $B_T=0.25\text{T}$ @ 0.64m
 $P_{RF}=0.2\text{MW} \times 2$
8.2GHz

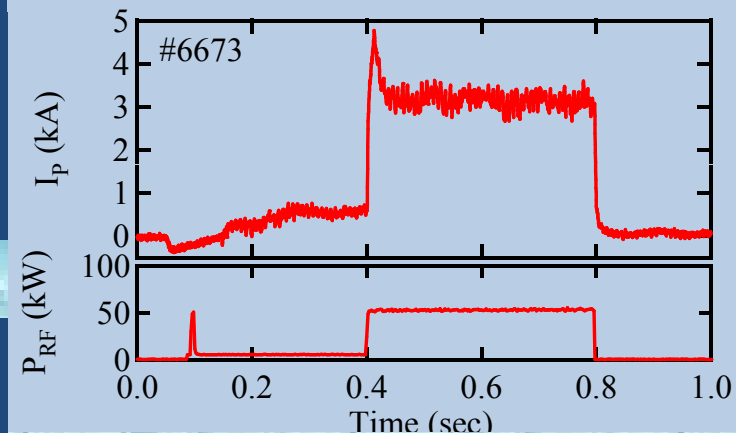
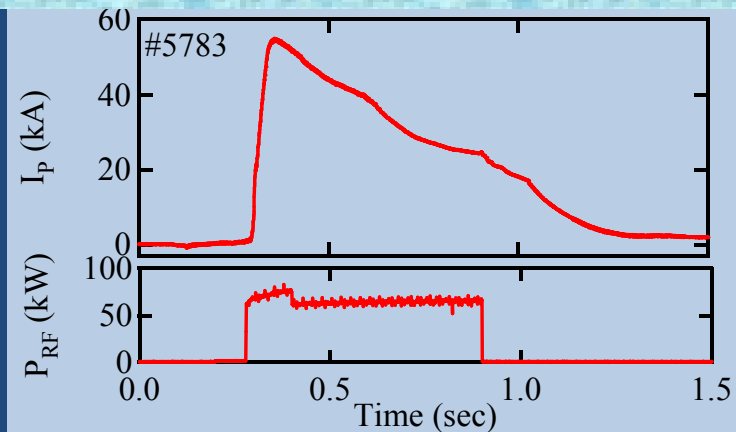
The experiments started on Oct. 2008.



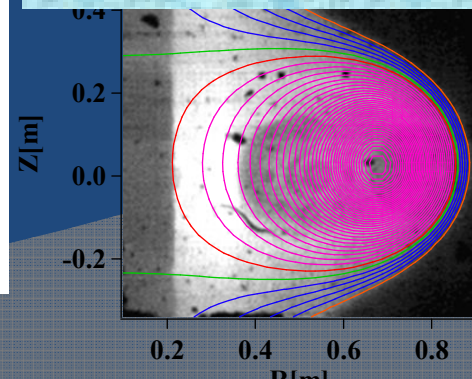
New Antenna for EBW and expected driven current



OH plasma and RF maintained plasma



Flux surface in OH + RF plasma

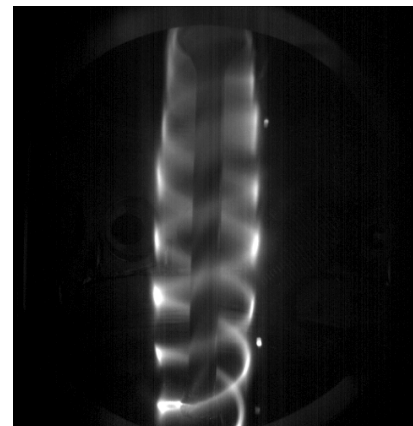


R=0.55m
a=0.3m
A=1.83
 $I_p=40\text{kA}$
 $B_T=0.15\text{T}$
 $P_{RF}=0.06\text{MW}$

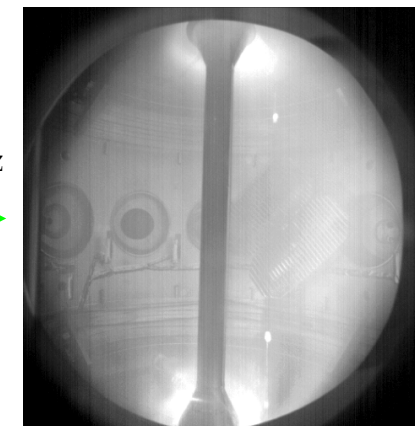


Local Plasma Current Sources + Helical Vacuum Field Give Simple DC Helicity Injection Scheme

- Current is injected into the existing helical magnetic field
- High I_{inj} & modest $B \Rightarrow$ filaments merge into current sheet
- High I_{inj} & low $B \Rightarrow$ current-driven B_θ overwhelms vacuum B_z
 - Relaxation via MHD activity to tokamak-like Taylor state w/ high toroidal current multiplication



Reduced B_z



$B_T = 10$ mT, $B_z = 5$ mT



Magnetic helicity injection is current drive

Magnetic helicity: linkage between magnetic fluxes

$$K \equiv \int \mathbf{A} \cdot \mathbf{B} \, dV$$

K is conserved in magnetized plasmas,
decaying on resistive timescales.



In tokamaks, K is proportional to the product $I_{TF}I_p$.
Increases in K correspond to increases in I_p .

Driving current on open field lines is helicity injection



DC helicity injection startup on PEGASUS utilizes localized washer-gun current sources

- Plasma gun(s) biased relative to anode:

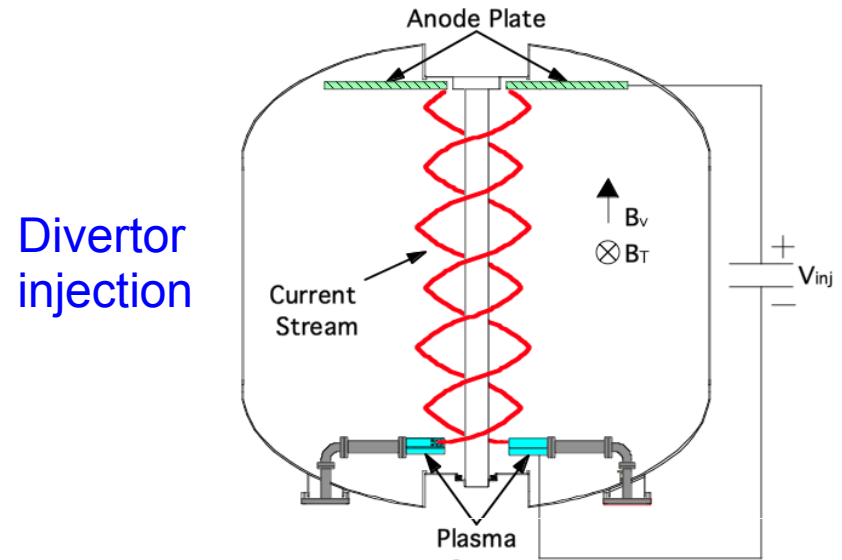
- Helicity injection rate:

$$\dot{K}_{inj} = 2V_{inj}B_N A_{inj}$$

V_{inj} - injector voltage

B_N - normal B field at gun aperture

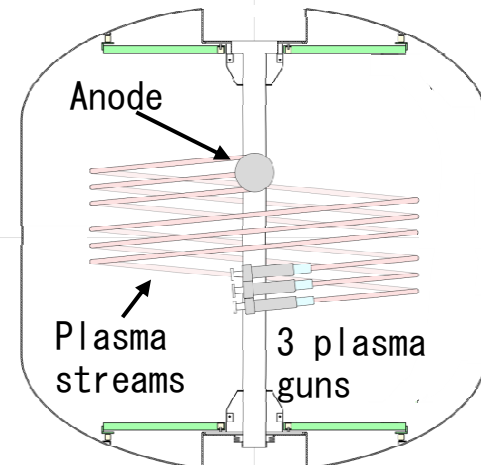
A_{inj} - injector area



Divertor
injection

- Plasma guns have geometric flexibility

Midplane
injection





Taylor relaxation criteria also limits the sustainable I_p for a given magnetic geometry

Helicity balance in a tokamak geometry:

$$\frac{dK}{dt} = -2 \int_V \eta \mathbf{J} \cdot \mathbf{B} d^3x - 2 \frac{\partial \psi}{\partial t} \Psi - 2 \int_A \Phi \mathbf{B} \cdot d\mathbf{s} \quad \rightarrow \quad I_p \leq \frac{A_p}{2\pi R_0 \langle \eta \rangle} (V_{ind} + V_{eff})$$

- Assumes system is in steady-state ($dK/dt = 0$)
- I_p limit depends on the scaling of plasma confinement via the η term

$$V_{eff} \approx \frac{N_{inj} A_{inj} B_{\phi,inj}}{\Psi} V_{bias}$$

Taylor relaxation of a force-free equilibrium:

$$\nabla \times \mathbf{B} = \mu_0 \mathbf{J} = \lambda \mathbf{B} \quad \rightarrow \quad \frac{\mu_0 I_p}{\Psi} \leq \frac{\mu_0 I_{inj}}{2\pi R_{inj} w B_{\theta,inj}} \quad \rightarrow \quad I_p \leq \left[\frac{C_p}{2\pi R_{inj} \mu_0} \frac{\Psi I_{inj}}{w} \right]^{1/2}$$

Assumptions:

- Driven edge current mixes uniformly in SOL
- Edge fields average to tokamak-like structure

A_p Plasma area

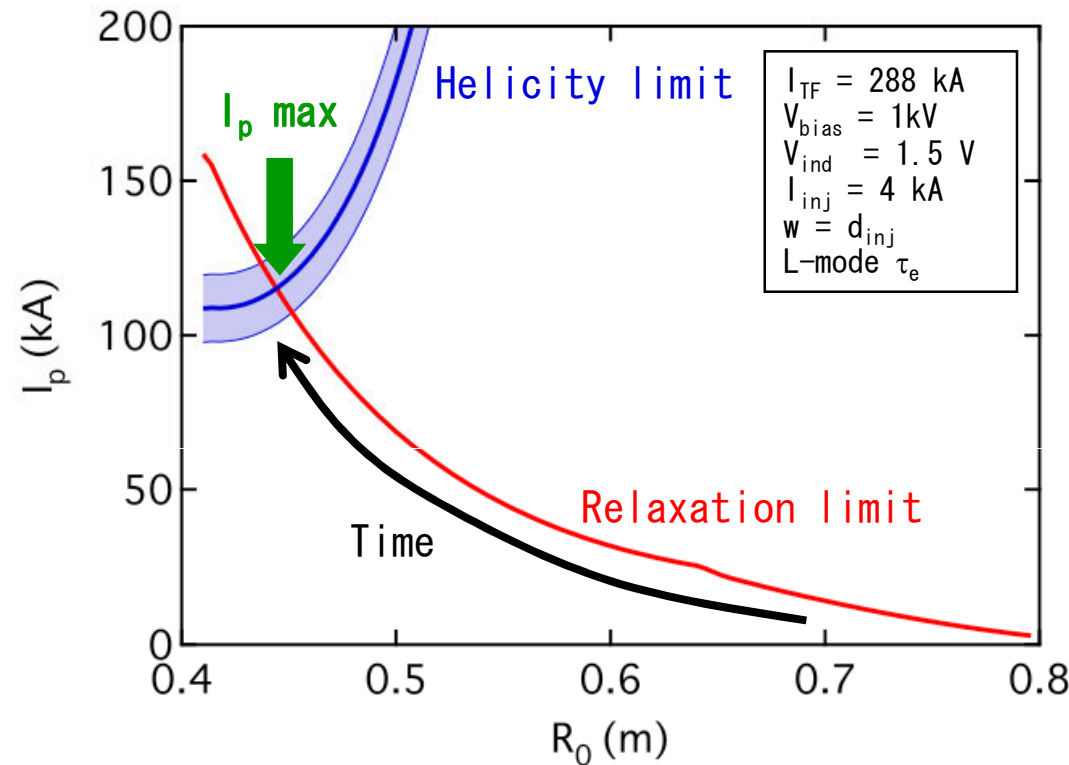
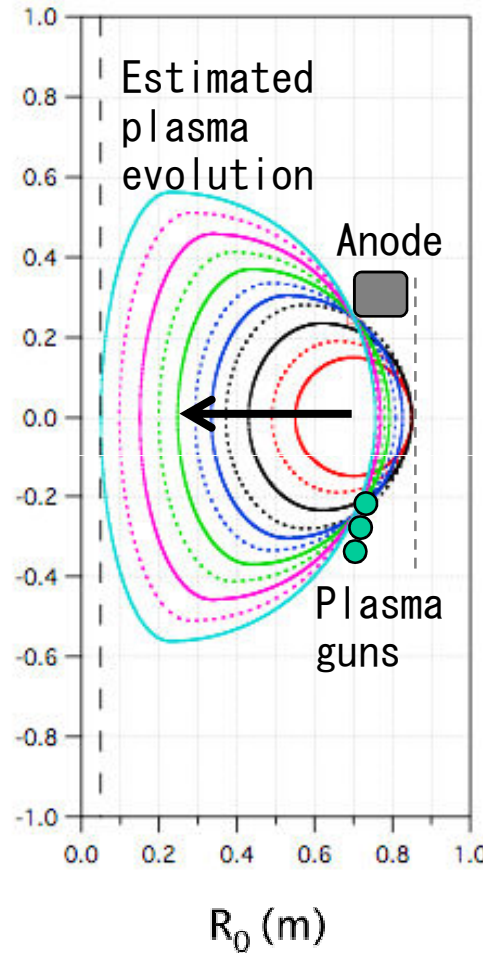
C_p Plasma circumference

Ψ Plasma toroidal flux

w Edge width



Maximum I_p achieved when helicity and relaxation limits are satisfied simultaneously



These particular parameters require a B_v ramp, both for radial force balance and some induction.

STを含めた核融合開発のロードマップ案

